2018

Comparative Analysis of Low Molecular Weight Fraction of Conditioned Media Derived from Starvation-Dormant and Anaerobically-Dormant Mycobacterium Avium Subsp. Paratuberculosis

Marina Buciuc
Minnesota State University, Mankato

Comparative Analysis of Low Molecular Weight Fraction of Conditioned Media Derived from Starvation-Dormant and Anaerobically-Dormant *Mycobacterium avium* subsp. *paratuberculosis*

By

Marina Buciuc

A Thesis Submitted in Partial Fulfillment of the

Requirements for the Degree of

Master of Science

In

Biological Sciences

Minnesota State University, Mankato

Mankato, Minnesota

July, 2018

July 2, 2018

Comparative Analysis of Low Molecular Weight Fraction of Conditioned Media Derived from Starvation-Dormant and Anaerobically-Dormant *Mycobacterium avium* subsp. *paratuberculosis*

Marina Buciuc

This thesis has been examined and approved by the following members of the student's committee.

Timothy E Secott, Ph.D.
Advisor

Rebecca J Moen, Ph.D.
Committee Member

Allison M Land, Ph.D.
Committee Member

ACKNOWLEDGEMENTS

First of all, I would like to express my deepest gratitude to my advisor Dr. Timothy Secott who inspired me to pursue career in research six years ago when I was taking his classes as an undergraduate foreign exchange medical student. Since then I could always count on his advice and guidance in my research which were indispensable for my program completion. Most importantly, however, I am thankful for his encouragements, good advice and impeccable sense of humor when my experiments hit the troubleshooting stage or when I felt lost. Dr. Secott is an outstanding professor who I had a pleasure to work with and learn from and I have witnessed dozens of students inspired to learn more under his guidance.

I would also like to express my gratitude to my committee members, Dr. Rebecca Moen and Dr. Allison Land. Despite their busy schedules, they have always found time to discuss my project, help with insightful advice, lend some biohazardous chemicals for my experiments, or assist with technology issues, e.g. move/ open centrifuge. I have also benefited from being their student and was impressed by their enthusiastic and efficient teaching style. A special thanks goes to Department of Biological Sciences who funded my study and provided everything I needed to complete my program.

Last, but by far not the least, I would like to thank my colleagues, Alexandra Grond and Sirri Ngwa, for making this experience fun and also helping me with some practical advice, Ron and Terri Prange for being my family away from home, and, of course, my parents and my sister who, though being very far, always have me in their thoughts.

Comparative Analysis of Low Molecular Weight Fraction of Conditioned Media Derived from Starvation-Dormant and Anaerobically-Dormant *Mycobacterium avium* subsp. *paratuberculosis*

Marina Buciuc

Master of Science in Biology

Department of Biological Sciences, Minnesota State University, Mankato, Mankato, MN

2018

ABSTRACT

Johne's disease (JD) caused by *Mycobacterium avium* subsp. *paratuberculosis* (MAP) is a contagious chronic enteritis affecting all ruminants and causing economic loss of at least $250 million annually in the US dairy industry. One of the major limitations in the diagnosis of JD is the low sensitivity of fecal culture in animals with no clinical signs of the disease, but who are actively shedding MAP. Persistence of MAP in the host with no apparent signs of infection is attributed to its ability to enter a dormant state wherein the bacterium is viable, but is not able to replicate until conditions become favorable. *In vitro* studies have shown that addition of culture media from starvation-dormant cells (SDCM) to growth media enhances the recovery of dormant cells. Resuscitative activity has been noted in the fraction of SDCM containing molecules equal to or smaller than 5kDa in size; the ability of this fraction to resuscitate was resistant to heat and enzyme treatment.

In this study we sought to further investigate the composition of low molecular weight fraction of SDCM in order to identify the nature of the molecules with resuscitative effect. Starvation-dormant MAP cells were grouped into three distinct

phenotypes based on acid-fast staining properties, and fractions of SDCM were obtained from cultures of similar phenotype. Only higher dilutions of fractions pooled from cultures with preserved acid-fastness had a resuscitative effect, which disappeared with higher concentration of the fraction. Fractions derived from cultures with complete or partial loss of acid-fastness either had no effect or inhibitory effect on MAP recovery. The concentrates of resuscitative fractions were comparatively analyzed with non-resuscitative fractions of SDCM, fractions of ADCM and growth media for protein/peptide concentration and lipid profile using BCA assay, SDS-PAGE gel electrophoresis, and thin layer chromatography. No proteins of 5kDa or smaller were detected in any of the samples. Resuscitative fractions of SDCM had a different mycolic acid profile compared to non-resuscitative, ADCM fractions, and cell-wall bound mycolic acids from exponentially growing MAP. Further analysis of lipid composition and lipid purification are needed in order to test whether lipids are involved in resuscitation of the MAP cells from the dormancy.

TABLE OF CONTENTS

LIST OF FIGURES AND TABLES

CHAPTER 1: INTRODUCTION

Johne's disease (JD), contagious chronic enteritis affecting most if not all ruminants, has been a burden for the dairy industry in the US (46, 47, 59) and across the world. It is caused by *Mycobacterium avium* subsp. *paratuberculosis* (MAP), a weakly Gram-positive acid-fast staining bacillus (69). Just as its notorious siblings, *M. tuberculosis*, *M.leprae*, and *M. bovis*, MAP persists in the host for years, provokes formation of granulomas, and is hard to eradicate. Once clinical symptoms develop such as decrease in milk production, intractable diarrhea, and wasting, the animal is considered to be fatally ill and is culled. MAP is primarily transmitted via fecal-oral route (48), animals being infected usually after ingesting contaminated by feces food or water. It has also been found in raw milk (30, 73), colostrum, and several studies have shown that it can be transmitted *in utero* (48) as well. Even though most of the animals get infected in calfhood, clinical symptoms usually develop in 2- to 5-year-old animals.

Johne's disease has a significant economic impact on dairy industry in the US (46, 47) and across the world (26). The National Animal Health Monitoring System (NAHMS) reported that based on the study in 1996 herds with a high prevalence of Johne's disease experienced an average economic loss of $227 per clinically diseased cow (80). Annual economic loss due to Johne's disease in the US dairy industry is estimated to be at least $250 million (46, 81) and continues to grow.

Besides being the cause of JD, MAP has been associated with a number of considered autoimmune or idiopathic at this moment human pathologies such as Crohn's

disease (50), multiple sclerosis (MS) and neuromyelitis optica spectrum disorder (NOSD) (11). While MS and NOSD have been associated with increased numbers of antibodies to MAP peptides cross-reacting with human epitopes (11) and possibly causing the inflammatory reaction, Crohn's disease is characterized by clinical and morphological picture very similar to JD. Many patients diagnosed with Crohn's disease are indeed testing positive for MAP infection (50). Though it is not yet elucidated to which extent MAP contributes to the acquirement and/or exacerbation of the above mentioned diseases, early diagnosis of the infection and better understanding of the pathogen itself might be advantageous in preventing and/or management of these conditions. Reports detecting MAP in pasteurized milk (24, 60) question the safety of dairy products from diseased cows for human consumption.

At the moment, there is no cure (48) for Johne's disease, nor is there a vaccine that prevents infection with MAP (62). Therefore, early diagnosis is an important strategy for effective disease management. There are several tests available for detection of MAP infection; however, there is not a single *ante mortem* test that is both sensitive and highly specific. Up to this date, fecal culture remains the gold standard for MAP detection (88).

The advantages of fecal culture are high specificity, cost-efficiency, and simplicity of the method. However, whereas in clinically diseased animals sensitivity approaches 100%, it drops to 30%-50% in asymptomatic animals (88). Animals with earlier stages of the disease are less likely to transmit MAP due to much smaller bacterial load shed with the feces compared to an animal with clinical disease (48); hence, early detection and isolation of infected animals can significantly reduce JD prevalence in the

herds. However, current fecal culture protocols often fail to recover MAP from animals in the early stages of JD resulting in false-negative test results. It suggests that like other pathogenic mycobacteria (1, 3, 44), MAP might enter a dormant state that allows it to persist in the host for years, but makes it difficult to recover the bacterium in culture. Dormant mycobacteria can revert to actively-growing state when conditions become favorable again leading to the progression of the disease.

Based on the data acquired from studies on other pathogenic mycobacteria (1, 3, 44) , it is possible that difficulties in isolation of MAP from animals in early stages of the disease resulting in low fecal culture sensitivity is due to the dormant state of the bacterium present in feces. Therefore, it is important to assure resuscitation of the dormant MAP to decrease the number of false-negative test results. Identification of growth-enhancing factors and supplementation with them of growth media might be a way to overcome culturing difficulties and increase test sensitivity.

Studies on dormant *M. tuberculosis* have demonstrated the importance of Rpf proteins for reversion from dormancy (56, 93). It is predicted that Rpf proteins are able to break down peptidoglycan and possibly form second messengers (55) such as phospholipids, muropeptide Rv1174c and its cleavage products that have demonstrated resuscitative effect on dormant *Mtb* cultures (33, 92).

Other studies showed that the Rpf proteins might be a part of a resuscitative cascade and are dependent on initiating stimuli. Lipids have been studied as potential signaling molecules in the resuscitative cascade (70, 92). The role of lipids in dormancy

and resuscitation has been investigated by several research groups noting differences in mycolic acid composition of cell wall of dormant mycobacteria (3) and changes of expression of genes involved in lipid metabolism in dormant state (8, 36). Involvement of lipids in resuscitation was demonstrated by growth-promoting effect of free fatty acids on dormant *M. smegmatis* (70). Due to genetic similarity of MAP to above mentioned mycobacteria (33, 43, 93), it is reasonable to assume that similar growth-promoting factors are involved in its resuscitation; however, it yet needs to be demonstrated.

In vitro studies in our lab have shown that MAP is more likely to reverse from dormancy when a fraction of conditioned media (cell-free media from a previous culture) from starvation-dormant cells (SDCM) was added to the growth media (27). Resuscitative activity was noted in the fraction of SDCM containing molecules smaller than 5kDa in size, and the resuscitative effect of the fraction was resistant to heat and enzyme treatment (24) suggesting that a growth-promoting factor was not a protein, but not excluding the possibility of it to be a peptide or lipid. Similar fraction of conditioned media from anaerobically-dormant cells (ADCM) did not show any resuscitative activity (24, 27). **Therefore, the goal of this research project was to comparatively analyze low molecular weight fractions derived from starvation-dormant and anaerobically-dormant MAP in order to find differences in peptide and lipid composition.**

The objectives chosen to generate data to fulfill the above goal were to i) partition SDCM based on phenotype of dormant MAP culture determined by acid-fast staining and compare resuscitative effect of its low molecular weight fraction on anaerobically-dormant MAP; ii) use SDS-PAGE gel electrophoresis, Biuret and bicinchoninic acid

protein assays to determine presence of peptides in the concentrates of low molecular fractions of SDCM and ADCM; iii) use thin layer chromatography to compare mycolic acid and glycolipid profiles of low molecular weight fractions of resuscitation-promoting fractions of SDCM with other fractions of SDCM and ADCM.

Characterization of the factors promoting resuscitation will aid in their precise identification. This in turn may allow for bioengineering of these factors and supplementation with them of growth media leading to increased sensitivity of fecal culture method for early detection of MAP infection. Early and improved diagnosis will reduce financial losses attributed to Johne's diseases and will increase the safety of dairy and meat products for human consumption.

CHAPTER TWO: LITERATURE REVIEW

2.1 Johne's Disease

2.1.1 History

Johne's disease (JD), also referred to as paratuberculosis, is a contagious, chronic, granulomatous enteritis affecting most if not all ruminants. It likely has been affecting wild and domesticated ruminants for centuries; however, it was first mentioned in the literature in 1826 by d'Aroval, who reported a specific type of enteritis in some cattle with chronic diarrhea. Later in 1881, Hansen and Nielsen described morphological modifications of intestinal mucosa associated with Johne's disease, but it was not until 1895 when Johne and Frothingham described the disease and identified the presence of acid-fast bacilli in the specimen from the diseased cow in Germany. Based on the morphology of the bacterium and its ability to provoke the formation of granulomas, Johne's disease was mistakenly considered to be an atypical form of tuberculosis. However, after thorough evaluation of the disease, in 1906 Bang determined that *Mycobacterium tuberculosis* was not the causative agent and named the disease pseudo-tuberculous enteritis or Johne's disease (18, 48). In 1910 the etiological agent was isolated and named *Mycobacterium enteriditis chronicae pseudotuberculosae bovis johne* by Twort, and the disease often referred to as paratuberculosis. Since the year of its discovery the causative agent of Johne's disease was referred to as *Mycobacterium johnei*

and *Mycobacterium paratuberculosis*; however, nowadays, an accepted name is *Mycobacterium avium* subsp. *paratuberculosis*, hereafter referred to as MAP (18).

After the discovery of the first case in Germany, Johne's disease was reported in Denmark, France, Norway, the Netherlands, Belgium, later on encompassing all of Europe. The first documented case in the U.S. dates back to 1908 (14); since then Johne's disease has been reported in all states in the US. Johne's disease has been identified in Northern, Central and South Asia, Africa, Australia, New Zealand, South America. As of this date, it has not been reported in Antarctica (18, 48).

2.1.2 Economic and environmental impact

MAP can potentially infect all ruminants, including domesticated species such as cattle, goats, sheep, llamas, and wildlife species as deer, elk, etc. MAP can infect monogastric animals as horses, chicken, human and non-human primates as well. However, even though the bacterium is able to replicate, it rarely leads to progressive disease as in ruminants. Monogastric animals can still serve as shedders of MAP. Its wide host range makes it impossible to contain the disease; thus, the spread of the disease leads to economic losses and threat to biodiversity (32). The magnitude of economic loss depends on geographical region and its primary occupation.

In the U.S. Johne's diseases is the largest burden for dairy industry. As the disease progresses, the animals produce less milk, have to be prematurely culled, and the slaughter value is decreased (47, 59). The National Animal Health Monitoring System (NAHMS) reported that based on the study in 1996 herds with a high prevalence of

Johne's disease experienced an average economic loss of $227 per clinically diseased cow. NAHMS also reported that in 1996, twenty-two percent of US dairy farms had at least 10% of infected with MAP cattle (80), whereas based on 2007 Dairy NAHMS study 68% of dairy U.S. herds would report at least one MAP-positive animal. In large dairy herds, the prevalence of the disease would approach 100% (46, 81). Annual economic loss due to Johne's disease in the US dairy industry is estimated to be at least $250 million (47) and continues to grow.

2.1.3 Stages of Johne's disease

Johne's disease is a chronic disease with a slow course, with an incubation period ranging from less than 6 months to over 15 years. However, most often clinical symptoms develop in three- to five-year-old animals. Most of the animals get infected during calfhood and develop clinical paratuberculosis, described below, in 2-5 years. There has been an age-associated resistance to MAP noted, which might result from more mature immune system of adult animals. The course of the disease can be divided into four stages (17, 18, 32, 48).

Stage I is referred to as the initial, silent stage. Animals do not show clinical signs and do not shed detectable numbers of MAP. Stage I will primarily be found in youngstock and might take years to slowly progress to stage II.

Stage II, the subclinical stage, is characterized by healthy-appearing animals that shed low numbers of MAP. It is usually detected in older youngstock or mature animals; however, fecal culture or serologic testing is usually negative.

Stage III is considered to be clinical Johne's disease; however, some animals can still appear healthy. Clinical symptoms characteristic for this stage include acute or chronic diarrhea, weight loss despite normal appetite and reduction in milk production. Animals shed more than 10^{10} colony forming units (CFU) of bacteria per gram of feces into the environment, thus greatly contributing to the spread of infection within the herd (48). Johne's disease in stage III is often diagnosed clinically and easily confirmed by fecal culture or serologic testing.

Stage IV, the terminal stage, is characterized by emaciation, intractable diarrhea, and bottle jaw. Animals are culled for slaughter at this stage; however, the slaughter value is often decreased due to wasting or concerns regarding safety for human consumption (14, 17, 48).

When an animal in the herd is detected in stage IV of Johne's disease, further inspection of the herd will detect more animals at different stages of the disease. This phenomenon is referred to as "The Johne's Disease Iceberg" and depicts how Johne's disease is a hidden herd problem and affects a few generations at once. For every animal in stage 4, it is estimated that there are 2-4 animals in stage III, 3-8 animals in stage II, and 5-10 animals in stage I. Unfortunately, available testing will most likely not detect animals stage I and II, thus, greatly undermining estimates of the prevalence of the disease in a herd (14, 18).

2.2 *Mycobacterium avium* subsp. *paratuberculosis* (MAP)

2.2.1 Characteristics

MAP, the etiologic agent of Johne's disease, belongs to genus *Mycobacterium*, which includes weakly Gram-positive intracellular bacilli. MAP is 0.5µm in diameter and 1.5µm in length, and is a non-motile, non-sporeforming, obligately aerobic bacillus (69). One of the distinctive characteristics of the genus is the presence of mycolic fatty acids in the cell wall of the microorganism, which is responsible for acid-fastness of the bacteria, confers resistance to harsh environmental conditions, and may explain the long-term persistence of the organism in the host and the environment. At the same time, the thickness and decreased permeability of the cell wall limits the access to the nutrients, which is reflected by the slow growth rate of pathogenic *Mycobacterium* species. While the majority of mycobacteria are saprophytic and are only opportunistic pathogens, *M. tuberculosis*, *M. leprae*, *M. bovis*, and MAP cause chronic disease and are hard to eradicate once in the host (14). All pathogenic species are considered slow growers, with generation times between 12 to 24 hours. MAP is considered to have the slowest growth rate among mycobacteria, with generation time over 20 hours. Visible colony formation on solid media such as Watson-Reid agar or Herrold's egg yolk medium (HEYM) might require up to 4 months regardless the addition of various supplements and growth enhancing factors. MAP forms small, nonpigmented, rough colonies with complete margins and grows best at 37^{o}C (14, 48).

Besides slow growth, MAP is also a fastidious microorganism requiring addition of mycobactin, a siderophore, for growth. Many bacteria depend on certain metals for growth; however, pathogenic mycobacteria require organic iron. Mycobactins, internal sequestering agents, and exochelins, the external vectors, are known bacterial siderophores and are responsible for chelating and transporting iron. Mycobacteria are unique by having both siderophores present; however, most if not all of MAP strains lost their ability to synthetize mycobactin for culture. It explains the failure in earlier attempts to isolate MAP from parasitized host tissues. Though MAP can grow and multiply freely in the host, it requires addition of mycobactin when propagated in vitro (48). Mycobactin-dependence used to be a key factor of identification of a mycobacterium as MAP; however, after isolation of other mycobactin-dependent *M. avium* strains (69), it is no longer a defining criterion for MAP identification.

2.2.2 Classification

With over 170 recognized species of *Mycobacterium*, MAP belongs to *Mycobacterium avium* complex (MAC) which in its turn includes *Mycobacterium avium* and its subspecies, as well as *Mycobacterium intracellulare, Mycobacterium bouchedurhonense, Mycobacterium chimaera, Mycobacterium colombiense, Mycobacterium lepraemurium, Mycobacterium mantenii, Mycobacterium marseillense, Mycobacterium paraintracellulare*, and *Mycobacterium timonense* (35, 69). There are four distinguished subspecies of *M. avium: M. avium* subsp. *avium, M. avium* subsp. *hominissuis, M. avium* subsp. *paratuberculosis*, and *M. avium* subsp. *silvaticum* (69).

As with other mycobacteria, MAP possesses key characteristics of the genus: acid-fastness, the presence of mycolic acids containing 60-90 carbon atoms, and genomic DNA having guanine + cytosine content of the DNA of 61 to 71 mol%. Being a subspecies of *M. avium*, MAP shares about 90% of the genome with other subspecies; however, it can be distinguished from other subspecies of *M. avium* by the presence of multiple copies of an insertion element, IS900, absence of IS1245 in its genome (43), and its requirement for mycobactin supplementation in order to grow *in vitro*.

Molecular technologies applied in the last two decades allowed to distinguish two major groups of MAP strains: “Sheep-type” or “Type S” also referred as Type I and “Cattle- type” or “Type C” also referred as Type II. Original names for the types derived from the hosts of origin; however, they can be found in other mammals besides cattle and sheep. Each of the strains has multiple sub-lineages (74). MAP isolated from patients with Crohn’s diseases is grouped into Type C MAP (50). The two types can be distinguished from each other based on genomic variability due to specific large sequence polymorphisms (SNPs) including insertions, deletions, inversions, translocations, duplications, as well as host range, growth characteristics, and disease presentation. Generally, Type C is easier to isolate from clinical samples and can produce visible colonies in 4-6 weeks compared to Type S which takes 16 to 52 weeks to produce visible growth. Type S is also more sensitive to antibiotics including ampicillin and vancomycin, which might explain difficulties in its isolation (74). Normally, colony phenotype does not differ much between the strains, except that some strains isolated from sheep that can

produce yellow- or orange-pigmented colonies. Further genetic analysis of pigmented strains identified them as a sub-lineage of Type S (74).

2.2.3 Genome

The complete genome sequencing of MAP bovine isolate K-10 published in 2005 shed some light on a number of unique characteristics of the bacterium. The MAP genome is presented as a single circular sequence of 4,829,781 base pairs and G+C content of 69.3%. MAP contains a single *rrn* operon (16S-23S-5S) compared to two sets found in fast-growing mycobacteria. The presence of a single *rrn* operon is also characteristic for *M. tuberculosis*, *M. leprae*, and *M. bovis*, which further explains the slow growth rate of the above mentioned pathogenic mycobacteria. MAP K-10 genome contains 4350 open reading frames (ORF), which indicates that about 91.5% of the genome is translated into protein. More than 68% of the genes are homologues of those found in the etiologic agent of tuberculosis, *M. tuberculosis* (*Mtb*) (43).

The genome of MAP encodes for more regulatory genes than *Mtb* which might explain its ability to survive in a wider range of environmental conditions than *Mtb*. The dependence of MAP on mycobactin can be explained by a truncated form of *mbtA*, a gene in *mbtA-J* cluster that is responsible for mycobactin synthesis.

The MAP genome contains genes for nearly all major metabolic pathways; however, it is lacking *frdBCD*, which encodes fumarate reductase; *narX* which encodes a positive regulator for nitrate reductase, and *ureABC* and *ureDFG* which encode urease. The absence of these genes in MAP helps to distinguish it from other MAC species.

MAP shares some of the proteins associated with immunogenicity and virulence with *Mtb* such as PE/PPE family of proteins, proteins thought to be expressed on the cell surface. However, whereas these proteins comprise 10% of *Mtb* genome, they only account for 1% of that in MAP. This observation may suggest a less variable immune response to MAP and the potential efficacy of vaccines directed against these proteins compared to *Mtb* (43).

Another important gene related to pathogenesis is the mammalian cell entry (*mce*) gene, eight homologues of which were found in MAP. The mere presence of the gene does not confer pathogenicity as it is identified in non-pathogenic bacteria as well.

A total of 39 predicted proteins are unique to MAP and are lacking homologues in currently available databases. These proteins may have potential value for diagnosis of MAP infection (43).

Another distinctive feature of the MAP genome is the high number of repeat sequences and insertion sequences (IS) which serve as transposable elements. The MAP K-10 genome contains a total of 58 IS among which are 17 copies of the MAP-unique *IS900*, 7 copies of *IS1311*, and 3 copies of *ISMav2*. These sequences can serve as genetic markers of the bacterium (66, 75).

2.2.4 Transmission and spread

The route of transmission of MAP is mainly fecal-oral. Infected animals shed bacteria in their feces, contaminating the environment. MAP can survive in soil or water sources, thus, enabling the spread to new areas (89). An animal can get infected by

grazing in contaminated pastures or by drinking water containing MAP (48). It has been shown that MAP is present in raw cow milk (73) and colostrum, which may explain why most of the animals get infected in calfhood. It has also been shown that the offspring can get infected *in utero*. MAP may also survive milk pasteurization (24, 60), which might pose a threat of infection to humans.

2.2.5 Immunology and pathogenesis of MAP infection

The most common route of infection with MAP is through the gastrointestinal tract as a result of grazing in a manure-contaminated environment. Infective dose is believed to range between 10^3 to 10^4 MAP cells; however, clinical disease in sheep has been demonstrated with an infective dose of at least 10^8 MAP. Susceptibility to MAP infection and the magnitude of the infective dose depend on type of host, its age and immunological status, microenvironment, and the strain of MAP. Younger animals are considered to be more susceptible due to the immaturity of their immune systems (17, 32).

MAP passes the epithelial barrier of gastrointestinal tract through microfold cells (M-cells) that uptake foreign organisms and antigens in order to pass them to dendritic cells, macrophages, B-cells for antigen presentation to T-cells residing in Peyer's patches of the intestine. After being phagocytosed by a macrophage, MAP is not digested, nor does it lead to apoptosis of the macrophage (53). Like other mycobacteria, MAP is able to survive inside a macrophage by inhibiting acidification of phagosome and its fusion with the lysosome (40). Catalase and peroxidase are involved in neutralization of reactive

oxygen intermediates aimed to kill the bacteria, as well as alkyl hydroperoxidase reductase (AhpC), one of the major virulence factors of MAP, which inactivates both reactive oxygen and reactive nitrogen species (58). Thus, MAP provides for itself a shelter from circulating antibodies, NK-cells and T-cells by growing and replicating intracellularly.

The initial immune response generated by MAP infection is believed to be Th1-cell mediated, the goal being to kill the infected macrophage. However, failure to digest MAP or undergo apoptosis results in overproduction of cytokines such as IFN-ɣ, IL-1, IL-6, and tumor necrosis factor alpha (TNF-α) (64). Even though both serum and intestinal levels of cytokines are increased in subclinical animals, larger quantities are produced at the intestinal level. These cytokines are involved in granuloma formation, an attempt of the immune system of the host to wall off the infection and a pathognomonic sign of mycobacterioses. The expansion of these granulomas over time leads to establishment of cachexia (14, 48). Fluctuations in cytokine concentrations have a significant impact on the ability of MAP to survive intracellularly. Preincubation of murine macrophages with moderate levels of TNF-α (10 to 1,000 IU) improves survival, whereas higher doses of TNF-α (4,000 IU) significantly reduce bacterial numbers. Pretreatment of bovine monocytes with IFN-ɣ restricts intracellular growth of MAP (17, 18, 48).

Later in the course of the disease Th1-mediated immunity wanes and is replaced by Th2-mediated immune responses, with production of large amounts of anti- MAP antibodies. Unfortunately, since the pathogen is growing and replicating intracellularly,

these antibodies are of no use. Moreover, high titers of anti-MAP antibodies have been found in human patients with various autoimmune disorders suggesting that these antibodies might cross-react with host antigens (14, 18, 48).

Morphologically, overproduction of cytokines leads to continuous inflammation and recruitment of macrophages, T-cells and B-cells to the site of the infection enabling the formation of granulomas. Often, infected macrophages fuse together to form multinucleated giant cells. Granulomas lead to the thickening of intestinal wall which in its turn causes the reduction in the surface area and decreased nutrient absorption (18).

2.2.6 Survival of MAP in the environment

A nationwide US study that used standardized environmental sampling indicated that 68% of American dairy herds are infected with MAP (46). High herd prevalence of 35% or more was also reported from the UK, the Netherlands, Canada, Denmark, Ireland, and Australia (26). Epidemiological data implies that in order keep continuous rates of infection, MAP must survive harsh environmental conditions.

Multiple studies have shown that MAP can survive in highly alkaline environments (pH 12.4) for over 14 days, in feces -70^{o}C for more than 15 weeks, and in infected tissues mixed with compost at 80^{o}C for 90 days. MAP is somewhat sensitive to urine since it survives less than 30 days at 38^{o}C in feces containing urine (89). This might be linked to a lack of genes encoding urease in the genome. Moist environment also favors MAP survival; however, viable bacteria can be found in dried feces after over 47 months. MAP is more sensitive to direct sunlight, with several studies showing reduced

isolation of MAP in sunlight compared to organisms cultured from shaded environments. In case of MAP, it is believed to be the thermal flux from the sun rather than UV irradiation that has bactericidal effect (21, 89). MAP is also able to survive in sterile pond water over 9 months at room temperature and up to 163 days in a temperate climate (9).

Environmentally, JD is more prevalent in the pastures with higher clay content in the soil as well as acidic soils; whereas, aridic climate and alkaline soils are less favorable for MAP isolation. Many farmers practice lime addition to the pasture lands to reduce JD occurrence (21).

The ability of MAP to survive in such diverse and extreme conditions is attributed to the high content (60%) of mycolic acids in the cell wall that increase thickness and reduce permeability of damaging factors (89). However, the cell wall alone would not explain the ability of the bacterium to survive in nutrient-depleted conditions such as sterile pond water. Multiple studies have shown that MAP is able to enter a dormant state which allows it to survive without replicating (3, 89). Studies reporting formation of endospores by MAP failed to be replicated by other laboratories; however, a spore-like morphology of MAP has been described under nutrient starvation (41).

The impressive resistance profile of MAP indicates that it can persist in water systems even pretreated with chlorine (9). The heat resistance of MAP also supports the potential of MAP to survive milk pasteurization (24, 60). Thus, there are multiple sources available for human infection.

2.3 Management of Johne's disease

Johne's disease, once clinically manifested cannot be cured, nor can it be completely eradicated due to a very large host range including wildlife. Hence, the three major pillars in disease control are efficient management to decrease transmission, early diagnosis and culling, and vaccination (14).

2.3.1 Vaccination

Vaccination has been used as a tool for JD management since 1926 when Vallee and Rinjard developed the first vaccine consisting of a live non-virulent MAP and oil adjuvants (62). Since then many researchers directed their studies towards development of an effective live-attenuated vaccines. Live-attenuated vaccines are advantageous due to the cost efficiency of their production compared to subunit vaccines and their ability to generate both innate and adaptive immunity which can elicit protective response at the mucosal and systemic levels (28). Phage-mediated, transposon, and allelic exchange mutagenesis targeting virulence factors and genes necessary for survival is a commonly applied method for generation of attenuated bacterial strains. Examples of successful attenuated vaccine are *ΔrelA* mutant, WAg906 (*ΔMAP1566*), *ΔleuD* (22), *ΔsigL* (29), and *ΔsigH* mutants (28, 62).

Recently, Johne's Disease Integrated Program (JDIP) research consortium enforced a three phase vaccine candidate evaluation strategy. Phase I screens whether the vaccine candidate can induce monocyte derived macrophage (MDM) apoptosis; phase II

comprises a challenge test in a mouse model, and phase III evaluates the protective effects in a goat model (4, 62).

The biggest drawback of live-attenuated vaccines is their cross-reactivity with tuberculosis diagnostic tests and JD serological diagnostic assays. Thus, it might be challenging to distinguish whether positive skin tuberculosis test or JD serologic test is a confirmation of immunity or evidence of infection (39).

In order to overcome disadvantages associated with whole-cell based vaccines that include live-attenuated and killed vaccines, subunit vaccines have come into the market. Well-defined recombinant MAP proteins or DNA encoding immunogenic antigens will be able to generate antibodies highly specific to MAP. Studies showing decreased intracellular MAP growth in presence of high concentrations of IFN-ɣ make identification of antigens able to induce a strong Th1 response a priority (4, 31,76). Several antigens were tested as potential candidates for subunit vaccines: heat shock protein 70 (Hsp70) (38, 65), antigen 85 complex proteins (Ag85A, Ag85B, Ag85C) (64), alkyl hydroperoxide reductases (AhpC, AhpD) (58), superoxide dismutase, lipoproteins (LprG, MAP0261c), and PPE family proteins (MAP1518, MAP3184) (31). The Hsp70 vaccine demonstrated reduced bacterial load in vaccinated trial animals, lack of cross-reactivity with tuberculosis skin test, and serologic JD test (38, 65). However, vaccination with the Hsp70 vaccine did not yield the expected high levels of IFN-ɣ inducing B-cell activation instead, which puts under the question the sole role of Th1-immune response at early stages of paratuberculosis (6).

DNA vaccines have been effective in mouse models, and also are easy to store and are very stable (34). Viral vectors have been used to increase antigenic effects of DNA vaccines and provide high delivery of antigens to antigen presenting cells (12). However, DNA vaccines have been only tested in a mouse model. MAP can infect and replicate in small rodents, however, it usually does not cause pathology similar to ruminant disease (18); hence, the results of the mouse model studies cannot be directly translated to ruminants and have to be validated in an appropriate host.

At the moment, there are three commercially available vaccines, all three based on inactivated whole bacteria: Mycopar, Gudair, and Silirum (62). Only Mycopar (Boehringer Ingelheim Vetmedica Inc.) is approved for use in cattle in the United States and represents "MAP strain 18" which in fact is just a member of *Mycobacterium avium* species, but is not a MAP strain (62). Gudair (CZ Veterinaria, Spain) is based on heat inactivated MAP F316 strain adjuvanted with mineral oil and is used for sheep and goat vaccination. Gudair is used in Australia, however, longitudinal and cross-sectional studies produced unclear results regarding its efficacy (91). Silirum (Zoetis) is also based on MAP F316 and is recommended for cattle vaccination. Vaccination with Silirum led to reduction of the occurrence of clinical disease in farmed deer in New Zealand (26, 62).

Despite availability of vaccines that do show at least some level of efficacy (4), vaccination is not often practiced. One of the reasons is severe tissue damage at the injection site (39); however, the usage of highly refined mineral oils in Silirum is aimed to reduce granuloma formation. The major problem remains the cross-reactivity of available vaccines with diagnostic tests for tuberculosis and JD (39). In order to

overcome this drawback or a subunit vaccine should be invented, or diagnostic tests should become more specific.

2.3.2 Diagnosis

Despite the fact that the etiologic agent of JD has been discovered over a century ago, there is not a diagnostic test which is both highly specific and sensitive. All the available diagnostic tests can be split in two groups: the ones identifying the causative agent, and the ones identifying immune response. Negative test results do not exclude the infection, whereas positive test results, while more valuable from diagnostic point of view, can be lacking in specificity. In order to increase the sensitivity and specificity of the tests, many of the assays are used in combination. Serial testing has also been practiced based on slow course of the disease (32, 48).

2.3.2.1 MAP identification

Direct stain

Direct acid-fast staining can be done on feces in order to reveal mycobacterial bacilli. Ziehl-Neelsen or Wright's staining can also be applied to slide impression smears from tissues collected at necropsy or through a biopsy of the ileum and mesenteric lymph nodes. Direct staining, though being a rapid, simple and inexpensive method, has a very low sensitivity and makes it challenging to distinguish MAP from saprophytic mycobacteria (48).

Culture

Feces and tissue can be used to grow MAP in culture. MAP can grow in solid and liquid media as long as it is supplemented with mycobactin J. Commonly used media are Lowenstein-Jensen medium (LJ), Herrold's egg yolk medium (HEYM), and Middlebrook medium often supplemented with antibiotics and/or other selective agents. Conventional culture method takes on average twelve to sixteen weeks to detect visible colonies (48).

An alternative method is radiometric method of culture such as BACTECT 460TB. Instead of detecting visible colonies, the system monitors sample-inoculated bottles with media for ^{14}C-labelled metabolites produced by bacteria. A significant concentration of metabolites can be detected before the organism can form a colony, thus reducing detection time to as little as five weeks (90). Most radiometric methods use liquid media instead of slants, which also results in faster growth (30, 48). However, this type of testing can be performed only by specialized laboratories and requires handling and disposal of radioactive waste.

Another automated mycobacterial detection assay is the mycobacteria Growth Indicator Tube (MGIT) system which contains enriched Middlebrook 7H9 broth base and silicone beads embedded with an oxygen-sensitive fluorochrome. When oxygen is abundant, e.g. sterile media, fluorescence is quenched. As MAP grows, it consumes oxygen, thus increasing fluorescence which can be detected by naked eye or BACTEC MGIT 960 instrument (30, 48).

Liquid broth-based tests yield faster results than those using solid media; however, one should not forget that other microorganisms also grow better in liquid media. Rapidly growing organisms present in feces and tissues can easily contaminate and overtake over slow growing MAP resulting in a false-positive test result.

Fecal culture is considered a gold standard in MAP infection diagnosis, with specificity approaching 100% (88). However, since other mycobactin-dependent species of mycobacteria have been discovered, genotypic identification is recommended for the grown colonies. Despite high specificity, fecal culture has low sensitivity, which also varies based on the stage of the disease, host, and strain of the bacteria. It is also a very time-consuming process, which often needs to be repeated with a number of samples collected at different periods of time (68, 88).

Genotypic identification

Polymerase chain reaction (PCR) is used to amplify MAP DNA in clinical or environmental samples. The amplification target is usually unique to MAP insertion sequence IS*900*; however, IS*900* closely related elements are present in other mycobacteria such as *M. scrofulaceum, M. paraffinicum, M. marinum* (48), thus, reducing the specificity of the method. Different primer sets and protocols can be employed in the diagnostic laboratories in order to overcome this problem, as well as probing for other targets such as IS*1311, F57*, IS*MAP02*, and IS*Mav2* (66, 73, 75).

A triplex real-time PCR assay has been developed, which co-amplifies IS*900, F57,* IS*Mav2* using TaqMan fluorescent probes (66, 73, 75). This method can detect

MAP numbers as low as 10^2 CFU per gram of feces with the accuracy of 70%. The triplex real-rime PCR was found to be more specific, as compared with conventional IS*900* PCR (37).

Multiple real-time PCR probing for MAP2765c (target 251) and MAP0865 (sequence *F57*) genes (75) has been used for quantitative MAP detection in cattle gut tissue and in human tissue, and can be performed in less than 6 hours (16). Although specificity for multiple real-time PCR is higher, sensitivity usually decreases due to lower copy number of these targets compared to IS*900*.

PCR-based methods, when performed on colonies isolated from sample, approach 100% in both specificity and sensitivity. However, when applied directly to the sample, the effectiveness of PCR is significantly decreased due to diluted bacteria, presence of PCR inhibiting factors in feces or tissue, and microorganisms which might cross-react with probes (57, 61). Immunomagnetic separation, which is currently applied to milk samples, might improve the outcome of this method application (73). One should not forget, however, that PCR-based methods cannot distinguish between live and dead bacteria.

Enzyme restriction fragment length polymorphisms (RFLP) have been studied in strains isolated from different hosts from different countries in order to establish a standardized system for DNA fingerprinting of MAP strains. A study of 1088 strains digested with endonuclease *Pst I* and *Bst EII* revealed 28 RFLP types with no relationship between RFLP type and host species (48).

Antigen 85- monoclonal antibody immunoassay

Similar to hepatitis B surface antigen (HBsAg) detection widely used in screening for hepatitis B infection or immunity, an assay that can detect a unique MAP antigen would be a huge improvement in diagnosis. Antigen 85, a secreted product of replicating mycobacteria, though not unique to MAP, has been found circulating in blood, making it a good candidate for immunoassay (48, 64). Monoclonal antibody, which is highly specific for Ag85 and that can provide a sufficient level of sensitivity, will be able to detect infection without relying on immune response, which is the basis for currently available serologic tests. Immune response-based test results measuring the levels of cytokines or antibody titers vary depending on the stage of the disease and the ability of the host to generate a strong immune response. Most of the time, these are not very specific.

2.3.2.2 Evaluation of immunological response

Most infections cause the host to generate an immune response in order to fight or wall off the infection and prevent re-infection. It is usually manifested by increased levels of pro-inflammatory cytokines, clonal expansion of white blood cells, generation of antibodies with varying levels of specificity, recruitment of antigen presenting and immune cells to the sight of the infection, and cellular destruction via phagocytosis or apoptosis. Though there are trends in cytokine and antibody profile matched to certain agents, overall, those responses are not very specific with respect to MAP (48). Hence,

assays evaluating immune response are mostly applied for screening, and if positive, must be validated by a different test or histopathological and/or clinical findings (57).

Assays evaluating humoral immunity

There are three standard assays evaluating humoral immunity: agar gel immunodiffusion (AGID), complement fixation (CF), and enzyme-linked immunosorbent assay (ELISA) (48). Since their first application, many modified protocols and kits have emerged, but the principles remain the same.

AGID represents "passive diffusion of soluble antigens and/or antibodies toward each other and their eventual precipitation in a gel matrix" that can be visualized and interpreted as positive or negative result. The AGID is applied for voluntary disease surveillance in cattle, sheep and goats. Reduced sensitivity compared to ELISA has been reported in cattle. In order to avoid false-negative results, larger amount of antibody has to be used in order to yield results comparable to those from ELISA. However, the AGID seems to have better specificity (48). False-positive results in ELISA are often due to cross-reaction with other microorganisms that have similar epitopes, e.g. *Corynebacterium pseudotuberculosis* (18, 57).

The CF detects complement-fixing antibodies to MAP. The assay is often requested for international animal shipment health documents; however, both sensitivity and specificity of the test are lower than the AGID and ELISA (48).

ELISA is a rapid inexpensive way to detect antibodies in serum or milk of the animal. Commercially available kits allow performing the test by 'cow-side' without the

need to contract a laboratory (48). ELISA, in general, has a higher specificity and sensitivity compared to other assays assessing humoral immunity. When performed on samples from an animal with clinical stage of the disease, sensitivity and specificity are approaching 100% (88). However, ELISA has a low sensitivity in subclinical animals. Another drawback is the abundance of false-positive results due to cross-reaction of antibodies with other microorganisms (57, 88).

Assays evaluating cellular immunity

Mycobacterial infection triggers a cell-mediated response that can manifest as delayed-type hypersensitivity reactions. Skin testing, especially in young cattle, has been used to detect early infection. A purified protein derivative (PPD) of MAP is injected intradermally, and skin thickening over 3mm within 24 h -72 h is suggestive of infection. However, the test has a low specificity since it often provokes cross-reactions with other mycobacterial species and MAP vaccinates. Many MAP infected animals will react with PPD-B, which is used to detect infection with *M.bovis* (39). The comparative cervical test (CCT), in which both PPD-B and *M. avium* tuberculin (PPD-A) are injected, can be used to distinguish MAP-infected cattle from those infected with *M. bovis* (48).

An ELISA developed to measure concentration of a cytokine instead of an antigen is also among available diagnostic tests. It is used to determine the concentration of IFN-ɣ, a cytokine which is produced in large amounts during cellular immune response (54, 76). IFN-ɣ levels produced by peripheral blood leukocytes in response to stimulation by *M. bovis* antigens, *M. avium* antigens, and to a non-specific stimulant, e.g.

phytoheamagglutinin, are compared. The assay is commercially available; however, the low specificity and inconvenience of the assay limit its application (48, 57).

Histopathological and clinical diagnoses are also widely used, but they cannot be applied to early detection of the infection. The gold standard of MAP infection diagnosis is necropsy with histopathological analysis of intestinal tissue and isolation of MAP (57).

2.4 Dormancy

2.4.1 Definition of dormancy

The ability of MAP to persist in harsh environmental conditions, including the hostile environment of macrophages without a documented evidence of the ability to form spores suggests that, as with other mycobacteria, MAP can enter dormant state. Referred to by Wayne and Sohaskey as "non-replicating persistence" (NRP) (86), dormancy represents a reversible state of low metabolic activity which allows for survival of the microorganism without the need to replicate, and can be induced by unfavorable environmental conditions. The microorganism can revert to its actively-growing form once the conditions become again favorable for growth (44). Though dormancy is a viable state, dormant cells are often considered non-culturable due to difficulties associated with culturing these cells.

2.4.2 Models of dormancy

Dormancy and *in vivo* and *in vitro* dormancy model systems have been intensively studied for *M. tuberculosis (Mtb*) due to the tremendous clinical significance

of the organism and an important role attributed to *Mtb* dormancy in the pathogenesis of tuberculosis. Due to the genetic similarity between MAP and *Mtb* (33, 43) and related supporting experimental work, it is reasonable to assume that these models should also work to induce dormancy in MAP. Based on the *in vitro* nature of this thesis project, *in vitro* dormancy models will be briefly described.

The first *in vitro* induced dormancy experiment was performed by Corper and Cohn in the 1920s. *Mtb* cultures isolated from humans were sealed and incubated at 37^{o}C for 12 years, after which 0.01% viable organisms were isolated from the sediment of the bottles (1). Since then several models of induced dormancy have been developed based on three major pillars: gradual oxygen reduction also termed hypoxia, nitrous oxide treatment, or nutrient deprivation.

The most frequently cited model of hypoxia-induced dormancy was described by Wayne and Hayes in 1996. In the original model, cultures were incubated without agitation. This resulted in the generation of an oxygen gradient between oxygen-rich top and anaerobic bottom, allowing bacteria to gradually adapt to microaerophilic conditions and survive (85). However, in order to approximate the model to *in vivo* occurrence and induce dormancy through a temporal rather than spatial gradient, the model was improved by incubating cultures with agitation. The major shortcoming of Wayne's dormancy model is the lack of standardization and unexplained development of susceptibility to metronidazole (87) which was not found in *in vivo* experiments.

Starvation-induced dormancy was first published by Loebel el al. in 1932 (45); however, a modified Loebel nutrient-starvation model described by Betts et al. in 2002 (8) became more applicable. Nutrient depletion may mimic the physiology of the microorganisms within granulomas, in which nutrients become scarce. This type of dormancy has been induced *in vitro* by transferring microorganisms from nutrient-rich medium into nutrient-depleted medium, usually phosphate buffered saline (PBS) (1, 8). Dormancy was achieved once the respiration rate decreased to a level that could maintain viability, but could not support replication. Dormant microorganisms were then transferred back into nutrient-rich medium, where reversion from the dormant state was observed. The model described by Betts yielded *Mtb* with similar antibiotic resistance profile as dormant *Mtb in vivo* and did not confer metronidazole susceptibility as did Wayne's model (8).

Other models use nitric oxide (NO), an antimycobacterial compound produced by activated macrophages, to reversibly inhibit aerobic respiration and growth. As such, this is the anaerobic dormancy model (84). Other modified protocols allow for the evaluation of dormancy based on color changes of the redox indicators, e.g. resazurin (77).

Dormancy models have also been tested on other mycobacterial species such as *M. smegmatis, M. bovis*, and were able to induce NRP (3, 55,70).

2.4.3 Characteristics of dormancy

Dormancy is characterized by a low metabolic and respiration rates, and an overall reduction in protein expression (3, 36). The low respiration rate results in

diminished production of reactive oxygen species and reduced need for catalase synthesis. The near shutdown of metabolism allows for survival in a nutrient-depleted environment.

In the beginning of starvation-induced dormancy, lipid levels of normally lipid-rich mycobacteria drop; however, their synthesis resumes as starvation progresses. Lipid catabolism is explained as the adaptation phase, and rebound of its synthesis is the result of cell reprogramming and the rearrangement of cell wall lipid synthesis, e.g. that of mycolic acids. Carbon and energy needed for cell wall lipid synthesis in the dormant state are presumed to come from previously stored glycogen and trehalose molecules (3).

Prolonged starvation has qualitative and quantitative effect on mycolic acid synthesis, a major component of mycobacterial cell wall. There are three distinguished types of mycolic acids present in the cell wall: alpha mycolic acids, including at least 70% of all mycolates, gamma (keto-) mycolic acids (15%), and beta (methoxyl-) mycolic acids (10%). During starvation, total mycolate synthesis decreases; however, keto-mycolic acid synthesis is significantly increased, alpha-mycolic acid synthesis is also increased, but methoxyl-mycolic acid synthesis (responsible for wax ester formation) is slightly decreased. Keto-mycolic acids are straight-chain mycolates and can be more densely packed reducing cell wall permeability. Moreover, studies made on *M. smegmatis* showed that mycolates synthesized during starvation phase are modified during the synthesis, suggesting genetically reprogrammed mycolate class switching (3). Modifications in mycolate compositions might explain increased antibiotic resistance of

dormant mycobacteria through decreased cell wall permeability as well as overall increased resistance to hostile environments.

Starvation can also affect morphology of mycobacteria, particularly their acid-fast property, due to an overall reduction of the mycolic acid layer. Lamont *et al.* reported formation of spore-like morphology type of MAP which survived exposure to heat, lysozyme, and proteinase K. This phenotype was enriched on sporulating media (Arret-Kirshbaum agar), and transformed into acid-fast bacilli (41). However, sporulation in mycobacteria is a controversial topic and more data is needed to support sporulation as survival mechanism.

2.4.4 Resuscitation

Resuscitation is defined as the reversion from dormancy into an actively growing state, including the reconstitution of replication and metabolic activity. Whereas other bacteria use quorum sensing in order to regulate metabolism and population density control (63), this phenomenon has not been observed in mycobacteria. Studies trying to identify signaling molecules such as autoinducing peptides characteristic for Gram-positive bacteria or N-acyl homoserine lactones (13) produced by Gram-negative bacteria were not fruitful, leaving room for research to identify the mechanism of resuscitation in mycobacteria (81).

Several bacterial signals have been studied as putative signal molecules triggering resuscitation. The most well-researched signals at the moment are the resuscitation-promoting factor (*rpf)* genes which were first identified in *M. luteus* (55, 56) and later

found in other mycobacterial species including MAP (33, 93). *Rpf* genes (*rpfA-E*) were found to be necessary for resuscitation of *Mtb*, and, most likely, are functionally redundant and exhibit synergetic activity since deletion of at least several genes resulted in decrease of resuscitation. However, recent studies have shown that knockout of *rpfD* delayed reactivation in an *in vivo* murine model (82). The Rpf proteins most likely function intracellularly and exhibit properties of a dual lysozyme and lytic transglycosylase. Two of the Rpf proteins were predicted to be able to break down peptidoglycan and possibly form second messengers. These second messengers are thought to be phospholipids or muropeptides (55) such as Rv1174c isolated from *Mtb*. Peptide Rv1174c, 8kDa in size, had resuscitative effect on *Mtb*. Further proteolysis of Rv1174c yielded smaller peptides, 22 to 25 amino acid residues in length, which as well had resuscitative activity (92), suggesting that the small molecules can be the part of the resuscitative cascade.

Other studies show that the Rpf proteins might need other stimuli to initiate the cascade. Shleeva et al. demonstrated in their study of *M. smegmatis* resuscitative role of free fatty acids (FAs) with one or more unsaturated bonds including arachidonic acids. The resuscitative effect was achieved only within an optimal concentration range of FAs, with higher concentrations demonstrating inhibitory and /or toxic effect via cell membrane disintegration (70).

Another piece of evidence for the possible involvement of lipids in resuscitation is upregulation of *lipY* and *lipX* genes, encoding PE/PPE proteins, during resuscitation (36, 67). This resulted in the change of cell wall lipid staining pattern (7). Interestingly, most

of the other genes upregulated in dormancy stayed upregulated through resuscitation (36). A number of studies showed specific changes in expression of DNA repair genes and *clp* protease genes in resuscitation. The transcription factor ClgR regulates expression of *clp* genes together with expression of other transcription factors such as *sigH, sigE, dosR*. It has been noted that *sigH* and *sigE* are upregulated during resuscitation (36, 49). Surprisingly, the same study showed that aerobic metabolism and ribosomal genes were not co- upregulated with the *clp* protease and DNA-repair genes (49), suggesting multiple stages for the resuscitative process.

Most of the resuscitative studies were performed on *Mtb* or *M. smegmatis*, and even though MAP genome has homologs of above mentioned genes, their involvement in the resuscitation of dormant MAP remains to be demonstrated.

Previous research in our lab has shown that conditioned media from starvation-dormant MAP (hereafter referred as starvation-dormant conditioned media or SDCM) enhanced the resuscitation of anaerobically dormant and starvation-dormant MAP. Conditioned media derived from anaerobically-dormant MAP (ADCM) did not have effect on resuscitation (27). Further analysis of SDCM and its fractionation by ultrafiltration showed that only the fraction containing molecules of approximately 5kDa or less in size had resuscitative properties. The stability of resuscitative activity after treatment with high temperatures, digestive enzymes, and combination of digestive enzymes and heat favored the hypothesis that the molecule with resuscitative effect was not a protein (13), but this did not exclude the possibility of it being a peptide or lipid. Further analysis of the low molecular fraction of SDCM in comparison with ADCM will

help determine the nature of possible resuscitative molecule, and if identified, more targeted assays can be applied for its precise identification. Identification of resuscitative factors will allow to culture MAP even when dormant, thus improving the sensitivity of diagnostic fecal culture which in its turn will lead to better clinical and financial outcomes and better disease management. Hence, the nature of resuscitative properties of SDCM merits further investigation.

CHAPTER 3: MATERIALS AND METHODS

3.1 Preparation and collection of conditioned medium from starvation-dormant *Mycobacterium avium* subsp. *paratuberculosis* (MAP).

Mycobacterium avium subsp. *paratuberculosis* (MAP) PAMSUM8 (Minnesota State University, Mankato culture collection) was grown in M7H9C [Middlebrook 7H9 broth (Becton Dickinson, Sparks, MD) supplemented with 10% oleic acid-albumindextrose-catalase (Becton Dickinson), 0.05% Tween 80 (Sigma, St. Louis, MO), and 2 µg of mycobactin J (Allied Monitor, Fayetteville, MO) per ml]. MAP (1 ml) was grown in 9 ml M7H9C at 37^{o}C in sealed 25cm^{2} tissue culture flasks. Acid-fast staining was performed to check for contamination. After at least 8 months, MAP cultures were acid-fast stained again to check for contamination and cell morphology. Cells were harvested by centrifugation at 4192 x g at 4^{o}C for 30 minutes. The supernatant was collected and filtered through a 0.22 µm filter. This filtrate was used as starvation-dormant conditioned medium (SDCM) (27). The filtrate from the cells with similar morphology was pooled together and then transferred to Vivaspin 6 centrifugal concentrator with 5kDa ultrafiltration membrane cut-off (GE Healthcare, Little Chalfont, UK). The centrifugal concentrator was placed into collection tube and centrifuged in swinging bucket rotor at 2683 x g for 1 hour 45 minutes. The 5kDa ultrafiltrate then was syringe-filtered through 0.22 µm filter membrane into a sterile tube and stored at -80^{o}C until further use (13).

3.2 Preparation of anaerobically-dormant responder MAP

Anaerobically-dormant MAP responder cells were prepared by inoculating 200 µl of a mid- to late-exponential phase MAP into a 30 ml serum vial containing 20 ml M7H9C. The vial was closed with a rubber septum, sealed with an aluminum cap, and incubated at 37^{o}C for at least 3 months. Before MAP responder cells were collected, the viability of the culture was measured using the LIVE/DEAD BacLightTM - Bacterial Viability Kit (Molecular Probes, Eugene, OR) (52). The kit contains SYTO 9, which fluoresces green when bound to DNA and is membrane-permeant (staining DNA in all cells); and propidium iodide (PI), which fluoresces red when bound to DNA and is membrane-impermeant (displacing SYTO 9 in dead and dying cells). To collect cells for the viability assay, 100 µl of the dormant culture were withdrawn from the culture vial with needles fitted to 3 ml syringes, then put in an Eppendorf tube (13, 27). The Eppendorf tube was centrifuged at 1817 x g for 30 minutes. The pellet was collected and washed in 1 ml filtered phosphate buffered saline (PBS). The suspension was centrifuged again at 1817 x g for 30 minutes, and the dormant cell pellet was resuspended in 1 mL PBS. Three microliters SYTO 9 (1.67mM): PI (1.67mM) were added to the bacterial suspension and mixed by vortexing for three-5 seconds. The cell-dye suspension was incubated for 15 minutes in the dark and then analyzed by flow cytometry (Guava Technologies, Millipore). The percentage of cells fluorescing green only was recorded as the percent viability of the dormant MAP responder cells. Cells with highest percentage of viable cells ($\geq$ 50%) were used for resuscitative assays.

To collect anaerobically-dormant MAP responder cells, cultures were centrifuged at 1200 x g for 30 minutes at 4^{o}C. Cell pellets were collected and suspended in 3 ml sterile PBS with 0.05% Tween-20 (PBST). Cell suspensions were adjusted to 30% transmittance at 490 nm, which was equivalent to 2 x 10^{8} CFU/ml. Tenfold serial dilutions of the adjusted bacterial suspensions were used to obtain dormant cell concentrations of 2 x 10^{5} CFU/ml in 10 ml of M7H9C (13, 27).

3.3 Preparation of incubation chambers

Two pieces of benzylkonium chloride-soaked paper were placed inside a plastic sandwich container. The container was then autoclaved at 121^{o}C, 15 psi for 30 minutes and kept closed in a biosafety hood until use. To avoid contamination, the incubation chamber was exposed to UV light in the hood for 15 minutes prior to resuscitation assay setup or measurement of optical density (OD) (13, 27).

3.4 Assay for resuscitative effect of low molecular weight fraction of SDCM

Three twofold serial dilution of low molecular weight fraction of SDCM were prepared in M7H9C, and 100µl of 1:4 and 1:8 dilutions were added to hextuplicate wells of a 96-well microtiter plate. Anaerobically-dormant responder cells (100µl) were inoculated into all wells to a final concentration of 2000 CFU/well. Control wells contained only M7H9C and dormant responder cells (100µl of each), and blank wells contained only 200 µl of M7H9C. Microtiter plates were covered with a thin transparent polyester adhesive film (Whatman, Piscastaway, NJ) to minimize evaporation and contamination. The plates were then placed in the sterile plastic container and incubated

at 37^{o}C for 15 days. Every two days, plates were allowed to equilibrate to room temperature, plastic seals were replaced to remove condensation, and OD_{590nm} readings were obtained using a microplate reader (13).

All of the set up for resuscitation assays and preparation for OD measurements were performed aseptically in a biosafety hood. Fractions shown to promote a statistically significant increase in MAP growth compared to control were chosen for further analysis.

3.5 Absorbance spectrum

One hundred microliters of low molecular weight fraction of SDCM were analyzed across the entire wave length spectrum in order to determine the wavelength with most of the peaks. One hundred microliters of low molecular weight fraction of M7H9C were used as a blank.

3.6 SDS-PAGE gel analysis

Ten microliters of low molecular weight fraction of SDCM derived from cultures with different cell morphology, low molecular weight fraction of ADCM from three-month-old and one-year-old cultures, and low molecular weight fraction of M7H9C were prepared according to commercially available protocol using Orange G as a gel loading dye and loaded on two separate SDS-PAGE Mini- PROTEAN Precast gels (Bio-Rad Laboratories Inc., Bulletin 1658100) (10). One of the gels was stained with Bio-Safe Coomassie Stain, while the other was stained with Promega Silver Staining Kit (Madison, WI) (2) in order to reveal proteins.

3.7 Biuret Protein Assay

Samples of low molecular weight fraction of SDCM, ADCM, and M7H9C growth media, and bovine serum albumin were prepared according to commercially available protocol (25) in glass tubes. After 20 minutes incubation at RT, absorbance was measured at 540nm using a microplate reader. Protein concentration was calculated based on generated standard curve.

3.8 Bicinchoninic Acid (BCA) Protein Assay

One milliliter of low molecular weight fractions of SDCM, ADCM, and M7H9C growth media was lyophilized. All the samples were resuspended in 100 microliters of water. Bovine serum albumin was used to prepare standard curve. The samples and the standards were prepared in quadruplicate and analyzed in a 96-well microplate following instructions from PierceTM BCA Protein Assay Kit, Thermo Scientific (78). Protein concentration was calculated based on generated standard curve.

3.9 Thin Layer Chromatography (TLC)

3.9.1 TLC for detection of fatty acid/ mycolic acid methyl esters

Mycolic acids extracted from exponentially-growing MAP were used as a reference standard. MAP was inoculated in M7H9C [Middlebrook 7H9 broth (Becton Dickinson, Sparks, MD) supplemented with 10% oleic acid-albumindextrose-catalase (Becton Dickinson), 0.05% Tween 80 (Sigma, St. Louis, MO), and 2 µg of mycobactin J (Allied Monitor, Fayetteville, MO) per ml]. MAP (1 ml) was grown in 9 ml M7H9C at

$37^{o}C$ in sealed $25cm^{2}$ tissue culture flasks. Twenty five milliliters of exponentially-growing MAP were harvested by centrifugation at 1509 x g for 10 minutes at room temperature. The supernatant was discarded, and the pellet was resuspended in 5mL of water and centrifuged again. The supernatant was discarded and the bacterial pellet was transferred to a round-bottom borosilicate glass tube with phenolic screw cap. One and a half milliliters of low molecular weight fraction of SDCM, ADCM, and M7H9C growth media were lyophilized and resuspended in 100 microliters of water and transferred to round-bottom borosilicate glass tube with phenolic screw cap. Two milliliters of tetrabutyl ammonium hydroxide (TBAH) were added to each tube, and the tubes were incubated overnight at $100^{o}C$ in a heating block to allow for fatty/ mycolic acid hydrolysis. The next day, the tubes were allowed to cool down to room temperature and methyl esterification was achieved by adding to each tube 4mL of CH_2Cl_2, 300µl CH_3I and 2ml of water. The tubes were mixed for 1 hour at room temperature (RT) on a rotator. The tubes were then centrifuged at 2054 x g for 10 minutes at RT, which separated the mixture into two phases. Upper phase was discarded, and 4mL of water were added to lower organic phase. The tubes were mixed for 15 minutes, followed by centrifugation at 2054 x g for 10 minutes at RT. The upper phase was discarded to waste, and the wash step was repeated two more times (20, 51). The lower organic phase then was dried by leaving the tubes open overnight in the fume hood. After the evaporation of the organic phase, 3mL of diethylether were added to each tube, and the tubes were sonicated in a water bath for 10 minutes at RT. The tubes were centrifuged at 2054 x g

for 10 minutes at RT, and the contents were transferred into a new glass tube (20). The diethylether was evaporated by leaving the tubes open overnight in a fume hood.

The residue was resuspended in 100µl of CH_2Cl_2. Fifteen microliters of each sample were loaded on a plastic TLC silica gel plate (Analtech, Catalog #158017) using 10µl capillary tube (Drummond Scientific). Fatty acid methyl esters (FAMES) and mycolic acid ethyl esters (MAMES) were separated by TLC using hexane/ethyl acetate (19:1, v/v) as the solvent. Once the solvent was 1.5cm away from the top of the plate, the plate was removed from the TLC tank, briefly dried, and placed back again for a second round of migration. After the second round of migration the TLC plate was allowed to dry, and then was sprayed with 5% ethanolic molybdophosphoric acid. The lipids were revealed by charring the plate with a heat gun until the bands became visible (20, 51).

3.9.2 TLC for detection of glycolipids

Glycolipids extracted from exponentially-growing MAP were used as a reference standard. MAP was inoculated in M7H9C [Middlebrook 7H9 broth (Becton Dickinson, Sparks, MD) supplemented with 10% oleic acid-albumindextrose-catalase (Becton Dickinson), 0.05% Tween 80 (Sigma, St. Louis, MO) and 2 µg of mycobactin J (Allied Monitor, Fayetteville, MO) per ml]. MAP (1 ml) was grown in 9 ml M7H9C at 37^{o}C in sealed 25cm^2 tissue culture flasks. Twenty five milliliters of exponentially-growing MAP were harvested by centrifugation at 1509 x g for 10 minutes at room temperature. The supernatant was discarded, and the pellet was resuspended in 5mL of water and centrifuged again. The supernatant was discarded and the bacterial pellet was transferred

to a round-bottom borosilicate glass tube with phenolic screw cap. Methanol was added at 10:1 of cell material weight (23). The contents were heated in a water bath at 65^{o}C for 5 minutes. After cooling to RT, chloroform was added to reach 2:1 chloroform: methanol suspension (42). The contents of the tubes were homogenized by sonication in a water bath at RT for 10 minutes (20). The samples were stirred at RT for 14 hours and then filtered to recover liquid phase (15). The solvent was washed by adding 0.2 volume of 0.9% NaCl, vortexing and centrifuging at 1048 x g for 20 minutes. Upper phase was removed by pipetting as much as possible. The inside wall of the tube was rinsed with 1.5mL of pure solvent upper phase (chloroform: methanol: water, 3:48:47, v/v; 0.29% NaCl) which was pipetted gently in order to avoid mixing interphase with lower organic phase. Remaining original upper phase and the rinse were removed, and the procedure was repeated twice. Lower phase and remaining rinsing phase were made into one phase by addition of methanol (23).

Lipid solution was evaporated overnight in a fume hood. One and a half milliliters of low molecular weight fractions of SDCM, ADCM, and M7H9C growth media were lyophilized. All the samples were dissolved in chloroform, and 15µl were loaded on a TLC plate with a 10µl capillary tube. Chloroform/methanol/water (60:12:1, v/v) were used as a solvent. After the solvent reached the top of the TLC plate, the plate was removed from the TLC tank, was allowed to dry and sprayed with 0.5% α-naphthol dissolved in 50% methanol. After the first spray had dried, the plate was sprayed with 50% concentrated sulfuric acid. The glycolipids were visualized by charring with a heat gun until the bands appeared (72, 83).

3.10 Data analysis

All results from the resuscitative assay were entered into GraphPad Prism statistical software (La Jolla, CA) for data analysis. Each treatment, including serial dilutions, was graphed and compared to the control. One-way analysis of variance (ANOVA) was used to look for the significant difference among the means of different dilutions in a fraction for each day of the experiment. Two-way ANOVA was used to look for significant differences among the means of different dilutions of all fractions. Kruskal-Wallis tests were performed instead of ANOVA if the data were not normal. Dunnet's multiple comparison test and Tukey's Honest Significant Difference (HSD) test were used for post-hoc analysis of the data. Resuscitative effect was also assessed by analyzing whether a well reached optical density equal or greater than the mean of the control wells with three standard deviations added and maintained until the end of the experiment in order to correct for scanning error.

Images of TLC plates and SDS-PAGE gels were analyzed with ImageJ software (NIH, Bethesda, Maryland).

CHAPTER 4: RESULTS

4.1 The effect of dormant state on cell morphology

Starvation-dormant MAP cells after 8-month-long incubation at 37^{o}C were acid-fast stained with Ziehl-Neelsen reagents in order to check for contamination and cell morphology. Short bacilli with tendency to clump were observed on all slides. However, three phenotypes were distinguished based on acid-fastness. Some bacteria preserved their acid-fastness completely; the second phenotype represented a mixture of acid-fast and non-acid-fast bacilli, but with identical morphology otherwise; the third phenotype lost its acid-fastness, but resembled acid-fast MAP in shape, size and tendency to clump.

4.2 The effect of SDCM fractions from cells with varying morphology on dormant responder cells

SDCM from 8-month-old MAP cultures was collected and pooled together based on phenotype of the culture it came from generating seven batches labeled T1, T2, T3, T4, T5, T6, T7. T1 and T7 were pooled from cultures that retained their acid-fastness properties; T3, T4, T5 were pooled from cultures with mixed phenotype; T2 and T6 were pooled from cultures of non-acid-fast MAP. Low molecular weight fractions of all SDCM batches were obtained by means of centrifugal filtration through a membrane with 5kDa molecular weight cut-off (MWCO). Twofold serial dilutions of the low molecular weight fractions were prepared and tested for the ability to resuscitate three-month-old and 1-year-old anaerobically- dormant MAP. The optical densities at 590nm of responder

cells incubated with 1:8 dilutions of low molecular weight fractions of SDCM from acid-fast cultures (T1, T7) increased with increasing time of exposure. The growth stimulating effect was significant by day 4 ($p < 0.0001$) for T1 and by day 10 ($p < 0.001$) for T7 in both three-month-old and one-year-old responder cells. Assessment of resuscitative effect of the fraction by the number of positive wells that maintained optical density three standard deviations above the average optical density of the negative control wells until the end of the experiment also supported growth stimulating properties of 1:8 dilutions of T1 and T7. A 1:4 dilution of T7 increased the optical density of one-year-old responder cells ($p<0.001$), but not of the three-month-old cells. However, assessment of the resuscitative effect by the number of positive wells revealed only 2 positive wells out of 6; hence, the resuscitative effect of 1:4 dilution of T7 was considered not significantly different from the control.

Bacterial growth was inhibited compared to the control in wells treated with both dilutions of T5 and 1:4 dilution of T6 and T3 ($p<0.05$). Dilutions of other batches of SDCM yielded results that were not significantly different from the control ($p>0.05$).

4.3 Absorbance spectrum of low molecular weight fraction of SDCM

One hundred microliters of low molecular weight fraction of SDCM were scanned across absorbance spectrum in order to reveal a wavelength with a highest peak. One hundred microliters of low molecular weight fraction of M7H9C growth media were used as blank. The low molecular weight fraction of SDCM had the highest peak at 220nm, small peak at 260nm, and no peak at 280nm.

4.4 Analysis of low molecular weight fraction of SDCM for presence of low molecular weight proteins/peptides or amino acid polymers via SDS-PAGE gel electrophoresis and protein staining

Low molecular weight fractions of SDCM from T1, T2, T3, T4, T7, of ADCM from three-month-old and one-year-old cultures, and of M7H9C growth media were lyophilized and resuspended in smaller volume of water in order to generate 10X concentrates. The samples were loaded on SDS-PAGE gels using Orange G loading dye. The samples were stained with Coomassie Blue stain or silver nitrate in order to reveal proteins. No proteins of 10kDa or less in size were revealed in any of the samples.

4.5 Analysis of low molecular weight fraction of SDCM for presence of amino acid polymers via colorimetric techniques

Biuret and microplate BCA assays were performed to determine protein concentrations of the samples with bovine serum albumin (BSA) used to build standard curve. Both assays detect the presence of peptide bonds in the samples compared to Bradford that measures the presence of aromatic rings such as tryptophan, tyrosine, and phenylalanine. The Biuret assay was performed on non-concentrated low molecular weight fractions of SDCM and ADCM from three-month-old and one-year-old cultures. However, the results of the assay were inconclusive due to inability to generate a working standard curve (R= 0.7144). The BCA microplate assay generated a working standard curve (R = 0.9879). Samples for BCA assay were lyophilized and resuspended in small volume of water in order to generate 10X concentrates. According to BCA assay, all the

samples including fraction from growth media contained significant amounts of protein **(Table 4.1).**

Table 4.1 Protein concentration of 10X concentrates of low molecular weight fractions of SDCM, ADCM, and M7H9C growth medium determined by the bicinchoninic acid microplate assay (BCA).

Absorbance, 562nm	**T1**	**T2**	**T3**	**T4**	**T7**	**A3**	**A12**	**M**
Replicate 1	3.20	1.72	2.80	4.00	1.33	1.07	0.76	0.79
Replicate 2	3.36	1.69	2.64	4.00	1.20	1.11	0.82	0.82
Replicate 3	3.57	1.59	2.72	4.00	1.29	1.09	0.82	0.82
Replicate 4	3.53	1.57	2.58	4.00	1.17	1.06	0.77	0.76
Mean absorbance	3.42	1.64	2.68	4.00	1.25	1.08	0.79	0.80
[Protein], µg/ml	**3221.27**	**1449.5**	**2489.6**	**3805.2**	**1053.5**	**886.17**	**596.12**	**603.46**

T1, T2, T3, T4, T7 – low molecular weight fractions of SDCM from cultures with respective phenotype; A3, A12 - low molecular weight fractions of anaerobically-dormant conditioned media from three-month-old and twelve-month-old cultures, respectively; M – low molecular weight fractions of M7H9C growth medium supplemented with OADC.

4.6 TLC for detection of fatty acid/ mycolic acid methyl esters

Fatty acid methyl esters (FAMEs) and mycolic acid methyl esters (MAMEs) extracted from low molecular weight fractions of T1, T2, T3, T4, T7, ADCM (three-month- and one- year-old) and growth media were analyzed by TLC. FAMEs and MAMEs extracted from exponentially-growing MAP served as internal control. FAMEs

were present across all the samples including growth media. No MAMEs were detected in the growth media. All SDCM and ADCM samples had MAMEs present, but had different profiles. T1 and T7 had similar bands; however, bands in T7 were of lower intensity. MAMEs revealed in T1 and T7 were different from the ones present in exponentially-growing bacteria. Both samples of ADCM fraction had the same profile, but overall low concentration of MAMEs. Samples of SDCM from cultures with mixed phenotype (T3, T4) had identical profile and high concentration of MAMEs also found in internal control. Low molecular weight fraction of SDCM from non-acid-fast cultures (T2) had low concentration of MAMEs which differed from internal control and other fractions of SDCM and ADCM. Intensity of bands found on TLC was proportional to increase in protein concentration in BCA assay.

4.7 TLC for detection of glycolipids

TLC for detection of glycolipids revealed a band in internal control similar in migration pattern to lecithin, a phospholipid. Similar bands of a much lower intensity were observed in T1 and T7. Another band with a different migration pattern was detected in T1, but not T7. Glycolipids were detected in ADCM with a migration pattern more similar to phosphatidylethanolamine.

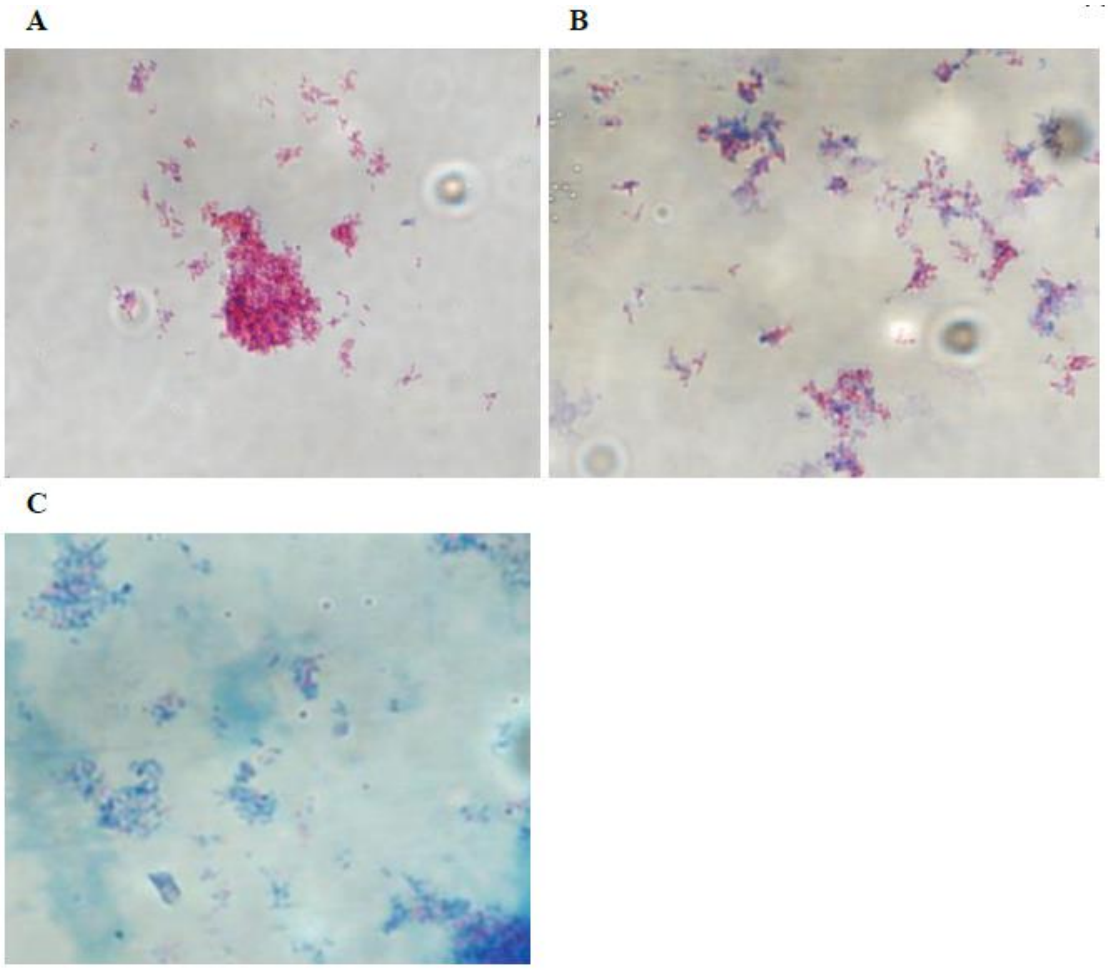

Figure 4.1 Three different phenotypes of 8-month-old starvation-dormant *Mycobacterium avium* susbsp. *paratuberculosis* (MAP) cells defined by Ziehl-Neelsen staining. A. MAP cells with preserved acid-fastness B. MAP cells with mixed phenotype C. Non-acid fast MAP cells.

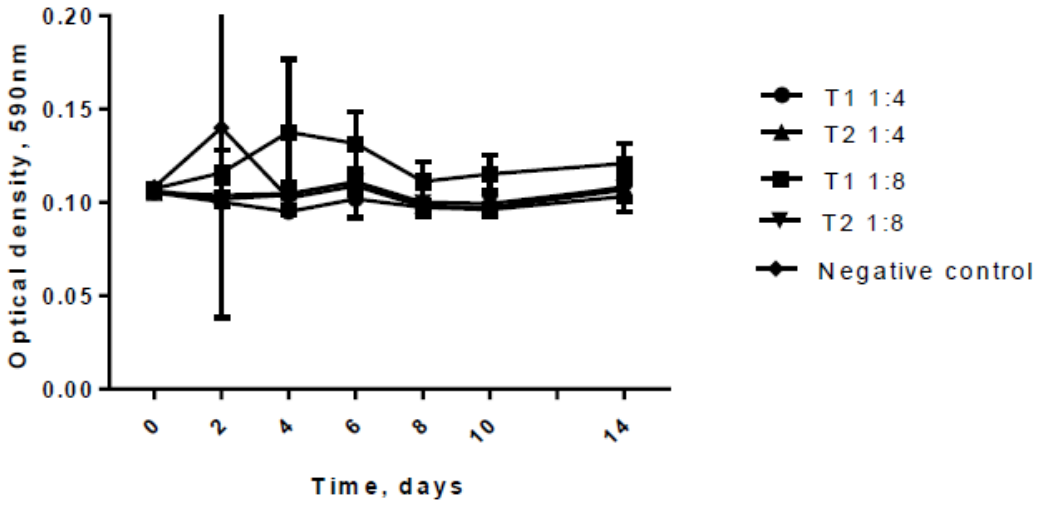

Figure 4.2 High dilution (1:8) of a low molecular weight fraction of conditioned medium from starvation-dormant MAP cells with preserved acid-fastness (T1) enhances growth of three-month-old anaerobically-dormant MAP cells. Twofold serial dilutions of low molecular weight fraction of SDCM (100 µl) were added to microplate wells containing 100 µl (2000CFU/ml) of anaerobically-dormant *Mycobacterium avium* subsp. *paratuberculosis.* T1 represents low molecular weight fraction of SDCM from acid-fast cultures, T2 – from non-acid fast cultures. Plates were incubated for 14 days and growth was assessed by optical density measurements (590 nm) every 48 hours at 590 nm. Control wells contained medium and dormant responder cells only.

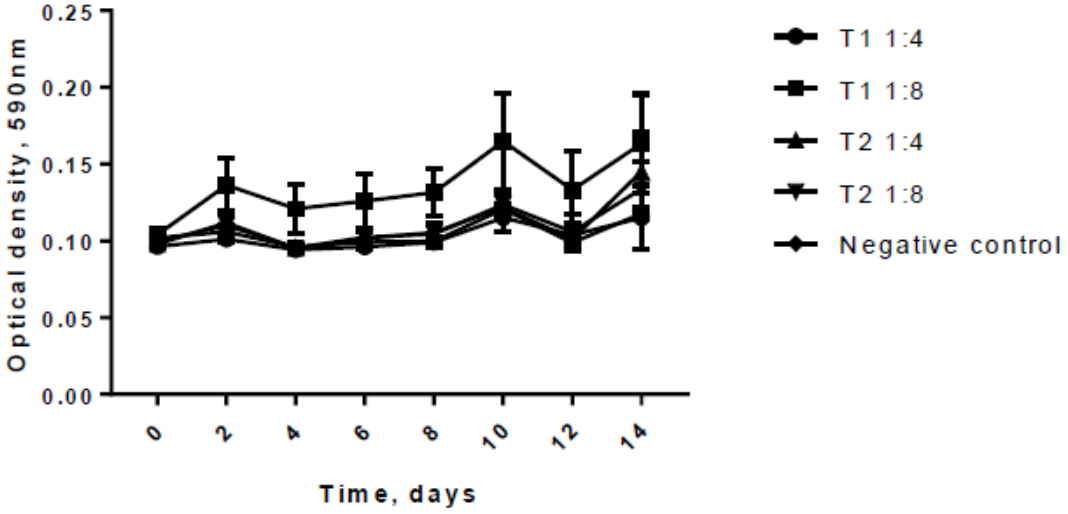

Figure 4.3 High dilution (1:8) of a low molecular weight fraction of conditioned medium from starvation-dormant MAP cells with preserved acid-fastness (T1) enhances growth of one-year-old anaerobically-dormant MAP cells. Twofold serial dilutions of low molecular weight fraction of SDCM (100 µl) were added to microplate wells containing 100 µl (2000CFU/ml) of anaerobically- dormant *Mycobacterium avium* subsp. *paratuberculosis*. T1 represents low molecular weight fraction of SDCM from acid-fast cultures, T2 – from non-acid fast cultures. Plates were incubated for 14 days and growth was assessed by optical density measurements (590 nm) every 48 hours at 590 nm. Control wells contained medium and dormant responder cells only.

A

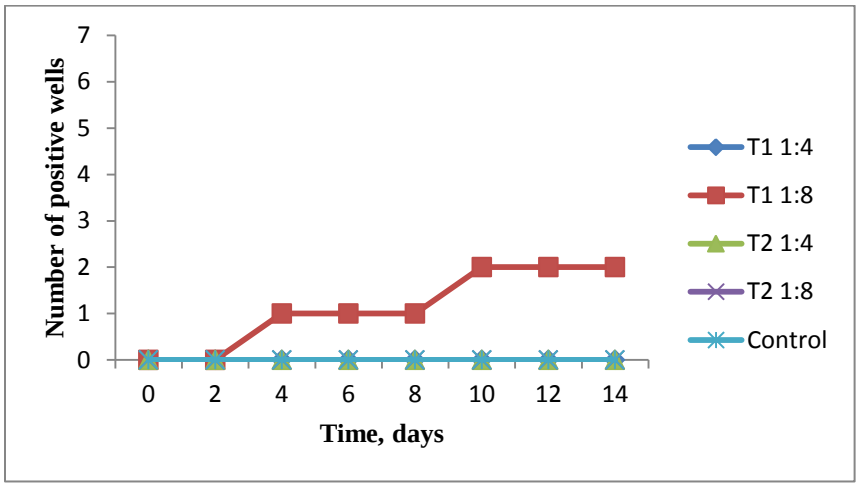

B

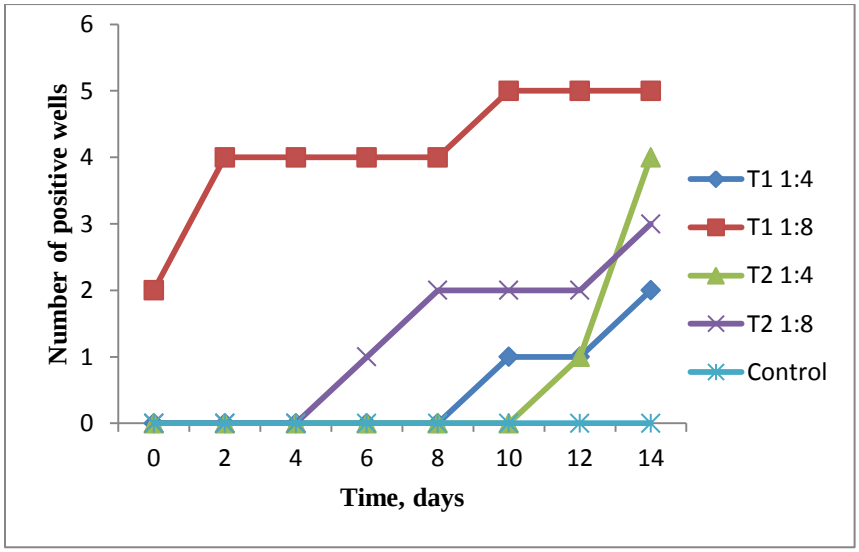

Figure 4.4 High dilution (1:8) of T1 has a resuscitative effect on anaerobically-dormant MAP cells. Positive well represents a well that reached optical density equal or greater than the mean of the control wells with three standard deviations added and maintained it until the end of the experiment. **A**. Resuscitative effect on three- month-old anaerobically-dormant responder MAP cells. **B.** Resuscitative effect on one-year-old anaerobically-dormant responder MAP cells.

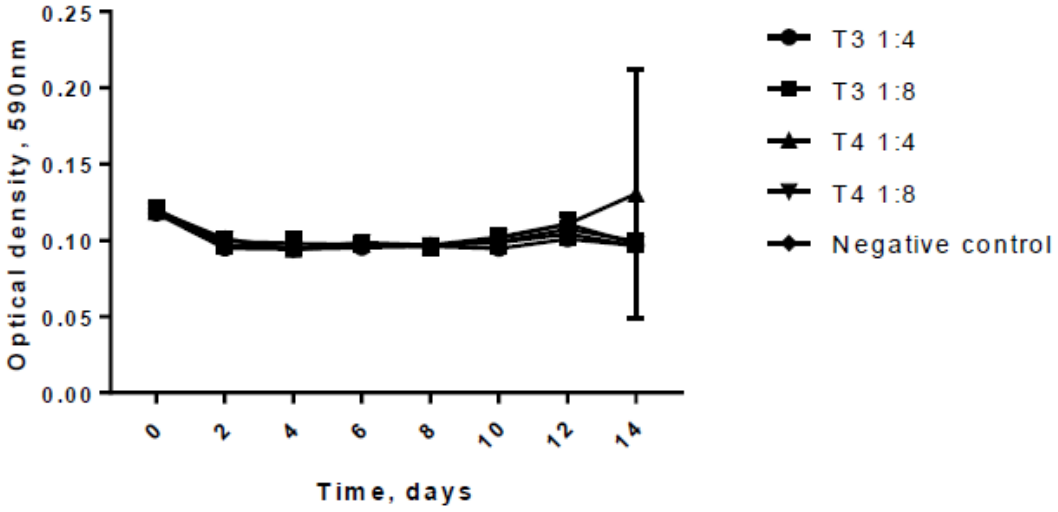

Figure 4.5 Low molecular weight fractions of conditioned medium from starvation-dormant MAP cells with mixed phenotype (T3, T4) do not improve the recovery of three-month-old anaerobically-dormant MAP cells. Twofold serial dilutions of low molecular weight fraction of SDCM (100 µl) were added to microplate wells containing 100 µl (2000CFU/ml) of anaerobically-dormant *Mycobacterium avium* subsp. *paratuberculosis.* T3 and T4 represent low molecular weight fraction of SDCM from cultures with mixed phenotype. Plates were incubated for 14 days and growth was assessed by optical density measurements (590 nm) every 48 hours at 590 nm. Control wells contained medium and dormant responder cells only.

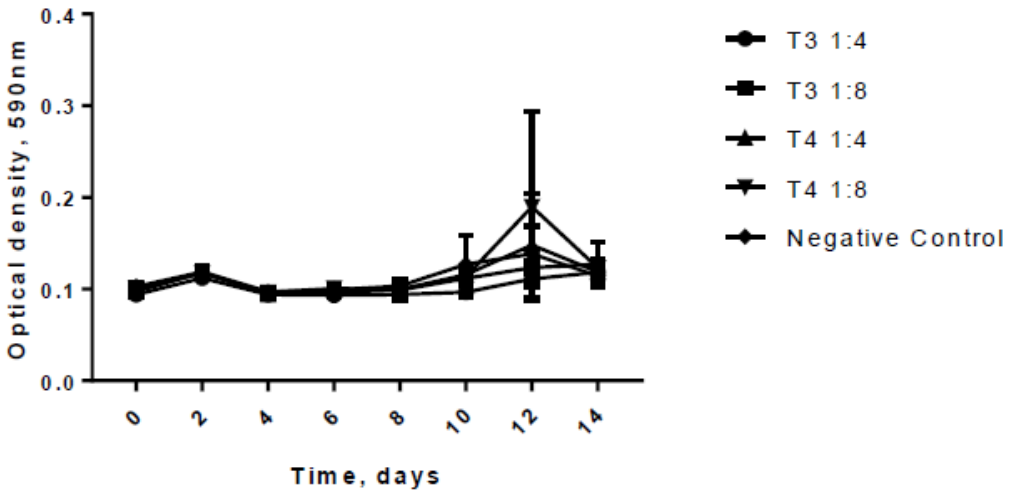

Figure 4.6 Low molecular weight fractions of conditioned medium from starvation-dormant MAP cells with mixed phenotype (T3, T4) do not improve recovery of one-year-old anaerobically-dormant MAP cells. Twofold serial dilutions of low molecular weight fraction of SDCM (100 µl) were added to microplate wells containing 100 µl (2000CFU/ml) of anaerobically- dormant *Mycobacterium avium* subsp. *paratuberculosis.* T3 and T4 represent low molecular weight fraction of SDCM from cultures with mixed phenotype. Plates were incubated for 14 days and growth was assessed by optical density measurements (590 nm) every 48 hours at 590 nm. Control wells contained medium and dormant responder cells only.

A

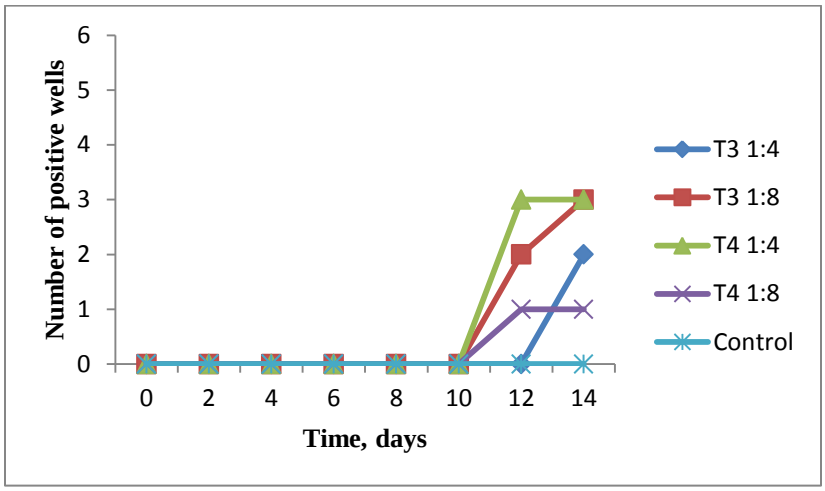

B

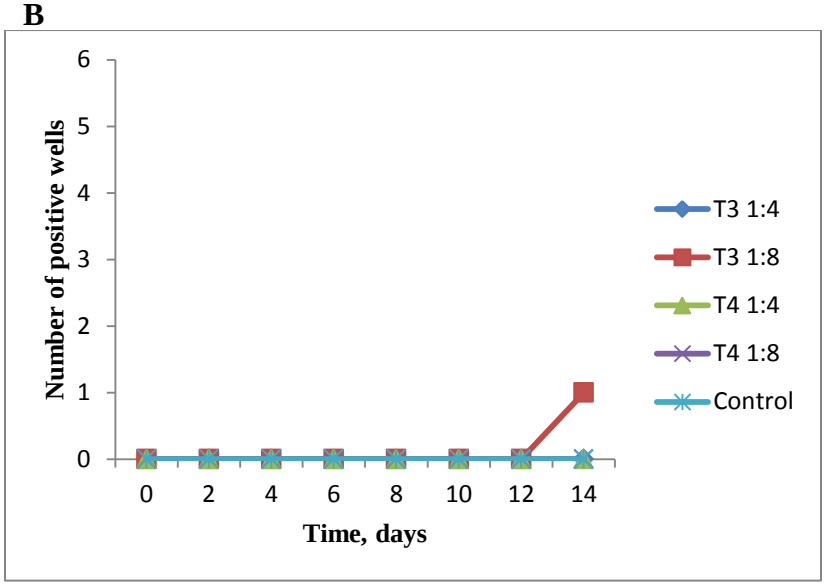

Figure 4.7 Addition of T3 and T4 fractions to the growth media does not improve recovery of anaerobically-dormant MAP cells. Positive well represents a well that reached optical density equal or greater than the mean of the control wells with three standard deviations added and maintained it until the end of the experiment. **A**. Resuscitative effect on three- month-old anaerobically-dormant responder MAP cells. **B**. Resuscitative effect on one-year-old anaerobically-dormant responder MAP cells.

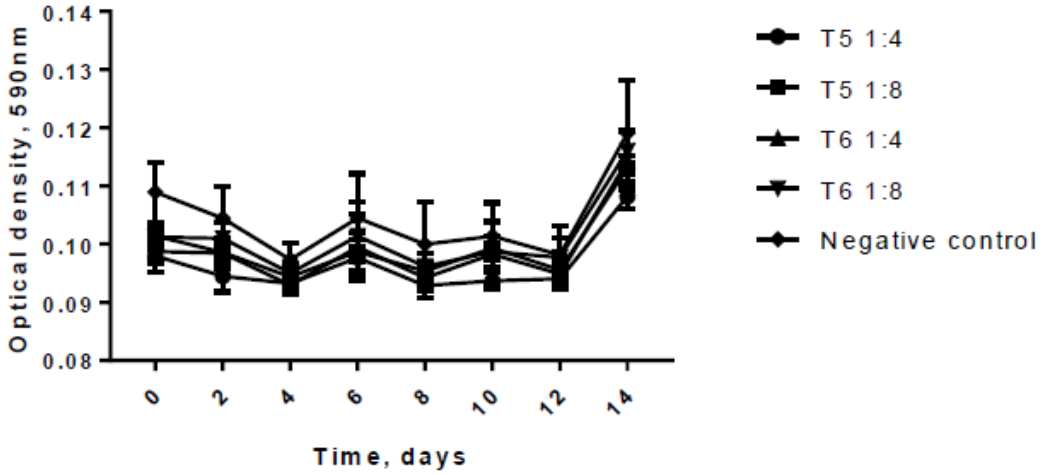

Figure 4.8 Low molecular weight fraction of the conditioned medium from starvation-dormant MAP cells with mixed phenotype (T5) and 1:4 dilution of low molecular weight fraction from starvation-dormant MAP cells with the loss of acid-fastness (T6) have inhibitory effect on recovery of three-month-old anaerobically-dormant MAP cells. Twofold serial dilutions of low molecular weight fraction of SDCM (100 µl) were added to microplate wells containing 100 µl (2000CFU/ml) of anaerobically- dormant *Mycobacterium avium* subsp. *paratuberculosis.* T5 represents low molecular weight fraction of SDCM from cultures with mixed phenotype, T6 – from non-acid fast cultures. Plates were incubated for 14 days and growth was assessed by optical density measurements (590 nm) every 48 hours at 590 nm. Control wells contained medium and dormant responder cells only.

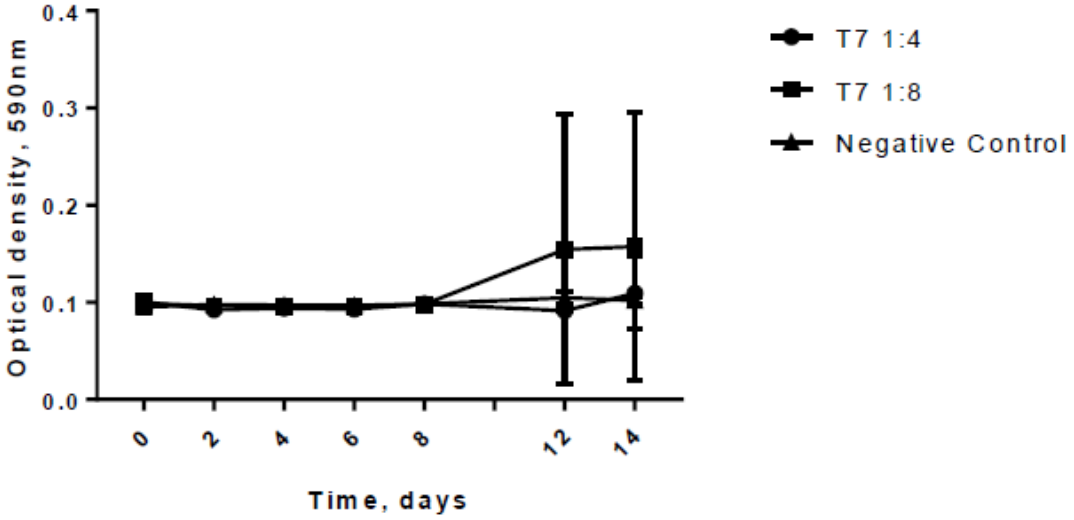

Figure 4.9 High dilution (1:8) of low molecular weight fraction of conditioned medium from starvation-dormant MAP cells with preserved acid-fastness (T7) has resuscitative effect on three-month-old anaerobically-dormant MAP cells. Twofold serial dilutions of low molecular weight fraction of SDCM (100 µl) were added to microplate wells containing 100 µl (2000CFU/ml) of anaerobically- dormant *Mycobacterium avium* subsp. *paratuberculosis*. T7 represents low molecular weight fraction of SDCM from cultures with preserved acid-fastness. Plates were incubated for 14 days and growth was assessed by optical density measurements (590 nm) every 48 hours at 590 nm. Control wells contained medium and dormant responder cells only.

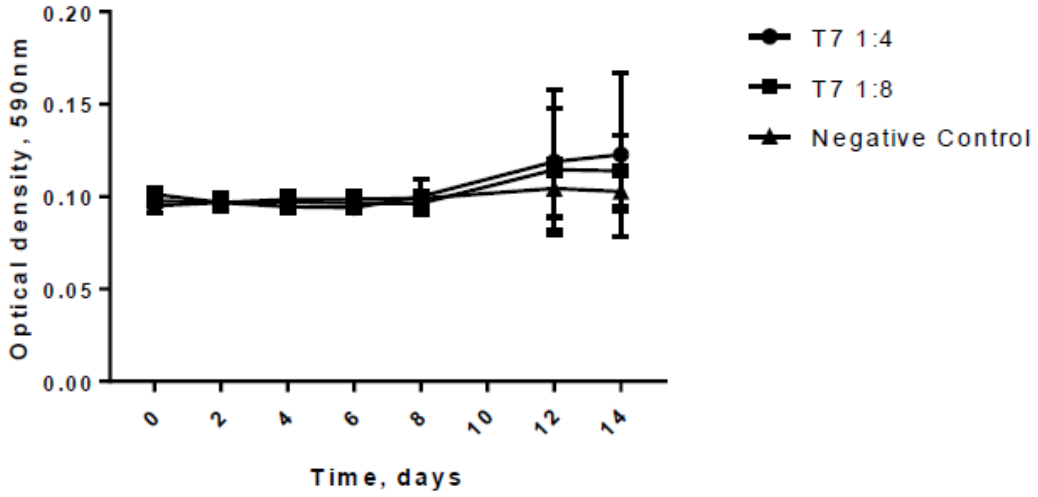

Figure 4.10 Low molecular weight fraction of conditioned medium from starvation-dormant MAP cells with preserved acid-fastness (T7) has resuscitative effect on one-year-old anaerobically-dormant MAP cells. Twofold serial dilutions of low molecular weight fraction of SDCM (100 µl) were added to microplate wells containing 100 µl (2000CFU/ml) of anaerobically- dormant *Mycobacterium avium* subsp. *paratuberculosis*. T7 represents low molecular weight fraction of SDCM from cultures with preserved acid-fastness. Plates were incubated for 14 days and growth was assessed by optical density measurements (590 nm) every 48 hours at 590 nm. Control wells contained medium and dormant responder cells only.

A

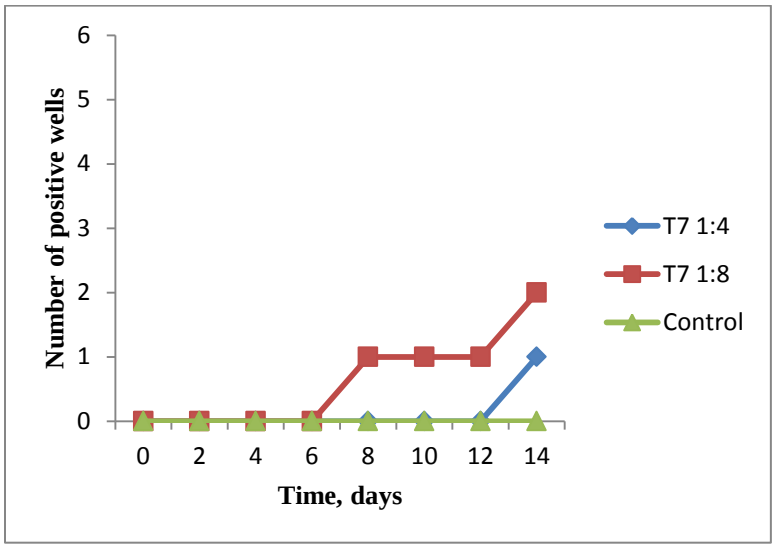

B

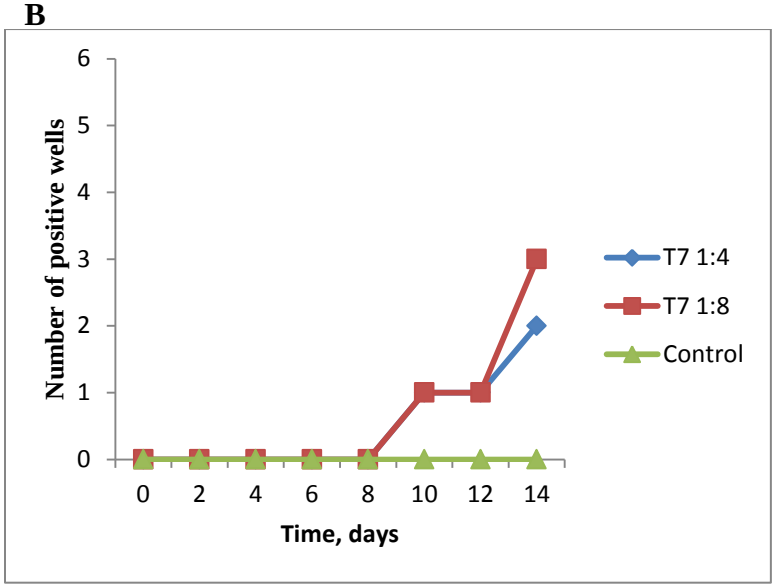

Figure 4.11 High dilution (1:8) of T7 has resuscitative effect on anaerobically-dormant MAP cells. Positive well represents a well that reached optical density equal or greater than the mean of the control wells with three standard deviations added and maintained it until the end of the experiment. **A**. Resuscitative effect on three-month old anaerobically-dormant responder MAP cells. **B**. Resuscitative effect on one-year-old anaerobically-dormant responder MAP cells.

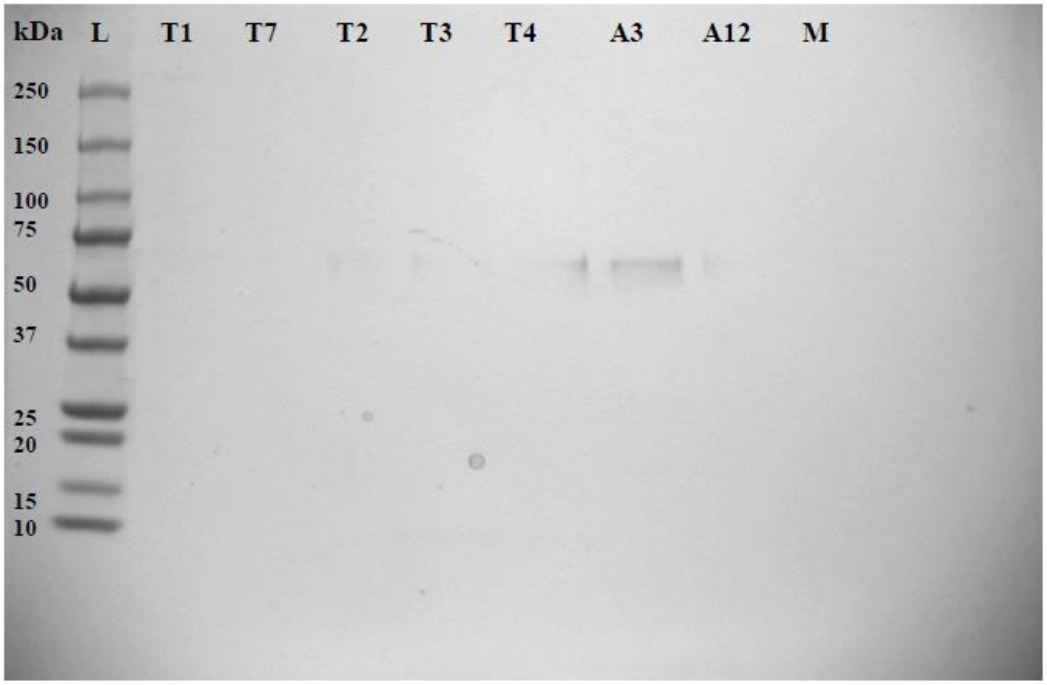

Figure 4.12 Concentrated (10X) low molecular weight fractions of SDCM, ADCM, and M7H9C growth media analyzed by Coomassie Blue staining of SDS PAGE gel do not contain detectable levels of low molecular weight proteins/peptides. Low molecular weight fractions of SDCM from T1, T2, T3, T4, T7, of ADCM from three-month-old and one-year-old cultures, and of M7H9C growth media were lyophilized and resuspended in smaller volume in order to generate 10X concentrates. The samples were loaded on SDS-PAGE gels using Orange G loading dye. The samples were stained with Coomassie Blue stain in order to reveal proteins. L – protein standard ladder; T1, T2, T3, T4, T7 – 10X concentrates of low molecular weight fractions of SDCM from cultures with respective phenotype; A3, A12 – 10X concentrates of low molecular weight fractions of anaerobically-dormant conditioned media from three-month-old and twelve-month-old cultures, respectively; M – 10X concentrate of low molecular weight fractions of M7H9C growth medium supplemented with OADC.

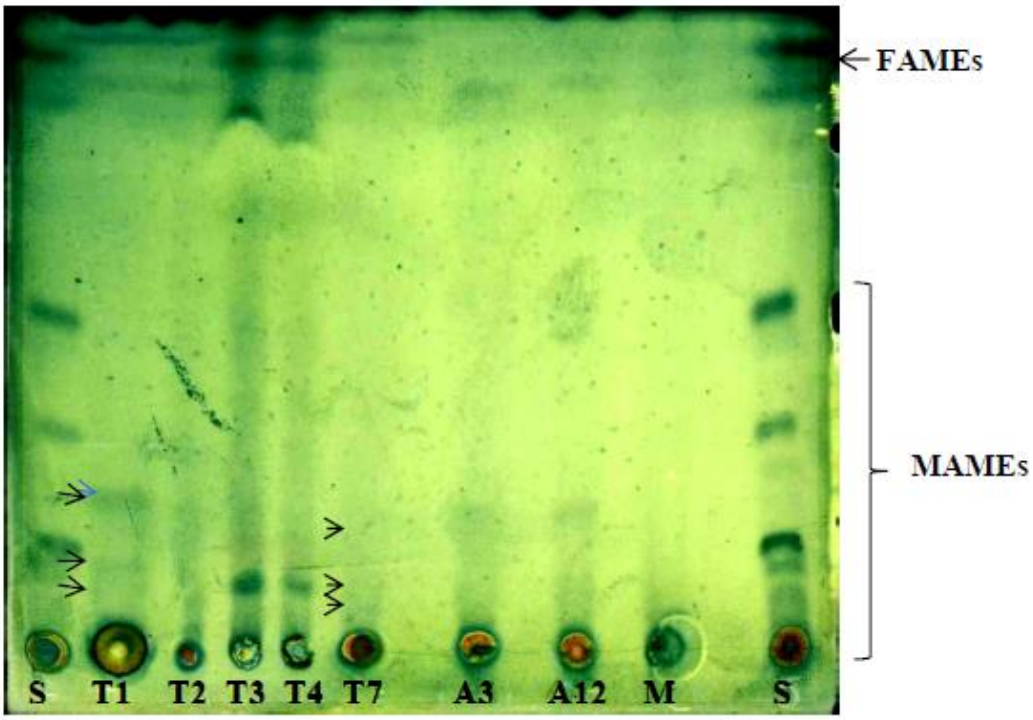

Figure 4.13 Chromatogram of fatty acid and mycolic acid methyl esters in 10X concentrates of low molecular weight fractions of SDCM, ADCM, and M7H9C growth media. FAMEs and MAMEs were extracted and analyzed by one-dimentional TLC using hexane/ethyl acetate (19:1, v/v, 2 runs) and revealed by spraying the plate with 5% molybdophosphoric acid followed by charring. S, FAMEs and MAMEs extracted from whole cell lysate of exponentially-growing MAP cells, served as internal control; T1, T2, T3, T4, T7 – 10X concentrates of low molecular weight fractions of SDCM from cultures with respective phenotype; A3, A12 – 10X concentrates of low molecular weight fractions of anaerobically-dormant conditioned media from three-months-old and twelve-months-old cultures, respectively; M – 10X concentrate of low molecular weight fractions of M7H9C growth medium supplemented with OADC. FAME, fatty acid methyl ester; MAME, mycolic acid methyl ester.

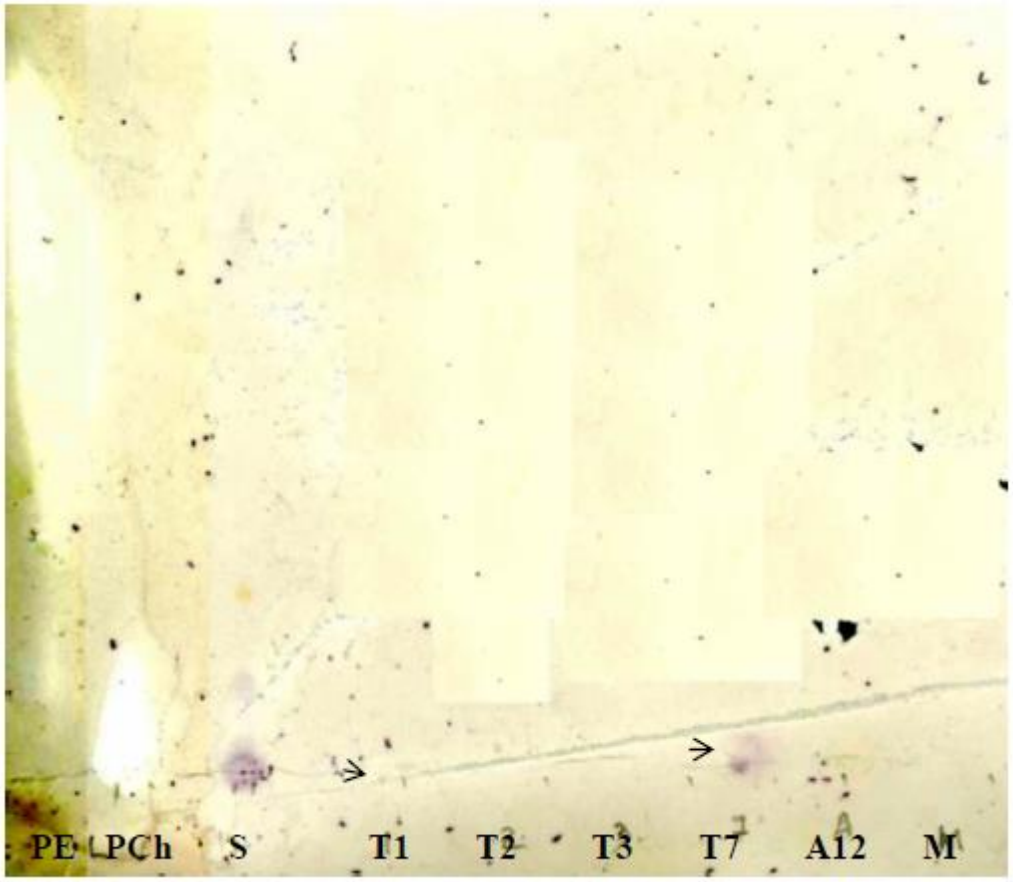

Figure 4.14 Chromatogram of glycolipids in the 10X concentrates of low molecular weight fractions of SDCM, ADCM, and M7H9C growth media. Lipids were extracted and analyzed by one-dimentional TLC using chloroform/methanol/water (60:12:1, v/v, 1 run) and revealed by spraying with 0.5% α-naphthol in 50% methanol, then with 50% concentrated sulfuric acid followed by charring. PE, phosphatidyl ethanolamine; PCh, phosphatidyl choline, served as reference phospholipids; S, lipids extracted from whole cell lysate of exponentially-growing MAP cells, served as internal control. Arrows indicate visible bands.

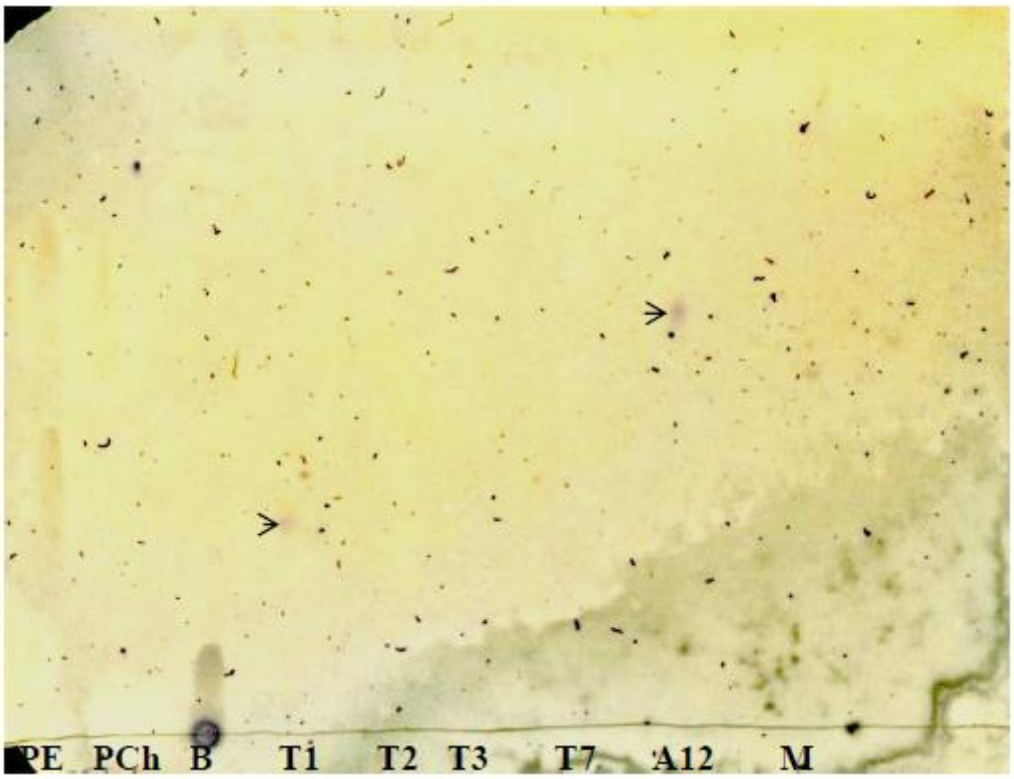

Figure 4.15 Chromatogram of glycolipids in the 10X concentrates of low molecular weight fractions of SDCM, ADCM, and M7H9C growth media. Lipids were extracted and analyzed by one-dimentional TLC using chloroform/methanol/water (60:12:1, v/v, 1 run) and revealed by spraying with 0.5% α-naphthol in 50% methanol, then with 50% concentrated sulfuric acid followed by charring. PE, phosphatidyl ethanolamine; PCh, phosphatidyl choline, served as reference phospholipids; S, lipids extracted from whole cell lysate of exponentially-growing MAP cells, served as internal control. Arrows indicate visible bands.

CHAPTER 4: DISCUSSION

Ante mortem diagnosis of Johne's disease is problematic due to low sensitivity and/or specificity of available assays, especially when testing animals in the subclinical stage of the disease (57). Fecal culture remains the most specific method of detection of MAP infection, with a relatively high sensitivity; however, the sensitivity of the assay drops drastically in animals with silent disease (88). Reduced sensitivity of fecal culture is believed to be due to inability to recover dormant organisms present in the specimen. Therefore, it is imperative to define the conditions that allow for the resuscitation of the dormant MAP in order to increase the sensitivity of the assay, improve disease management, and develop new diagnostic strategies.

Previous work by Ghimire showed that starvation-dormant MAP secretes substances that enhance resuscitation of anaerobically-dormant responder cells (27). Further investigation by Cao identified that resuscitative properties were attributed to low molecular weight fraction (< 5kDa in size) of SDCM. The low molecular weight fraction of SDCM was able to induce resuscitation of responder cells on its own in a dose-dependent manner; however, resuscitation was enhanced by the combination of the low molecular weight fraction of SDCM with fractions containing molecules ranging from 10kDa to 30kDa in size. Resuscitative effect of low molecular weight fraction was not diminished by heat exposure and/or digestive enzyme treatment (13). The present work aimed to further characterize the composition of low molecular weight fraction of SDCM

in order to determine the nature of the resuscitative factor. We observed different mycolic acid compositions in the low molecular weight fraction of SDCM having a resuscitative effect, compared to similar-sized fractions of ADCM, growth media, and SDCM with no resuscitative effect.

The phenomenon of dormancy has been observed in other mycobacteria, and potential resuscitative factors present in filtered conditioned medium have been described. The most studied resuscitation promoting factor is Rpf family of proteins with molecular weight of approximately 15-17kDa (56, 93). However, Cao's study did not find resuscitative effect of SDCM fraction containing molecules within 10-30 kDa range in size (13). The present study also has not detected bands of 15-17kDa on SDS PAGE gels of 10X concentrates of low molecular weight fraction of SDCM, nor has it identified peaks absorbing at 280nm characteristic for proteins and aromatic compounds. The bands at approximately 70kDa detected in certain fractions are most likely due to contamination with bovine serum albumin during lyophilization process since they were not present in non-concentrated samples. Hence, Rpf proteins are most likely not responsible for the resuscitative effect seen with SDCM.

A peak at 220nm observed in the absorbance spectrum of the low molecular weight fraction of SDCM suggested a peptide as a potential resuscitative factor. Zhang described resuscitative effect of Rv1174c peptide of 8kDa and its cleavage products of 22-25 amino acids in length on dormant *Mtb* (92). A homologue of Rv1174c, MAP2609 (GenBank accession number NP9615430) has been found in MAP genome. However, *in silico* digestion of Rv1174c or MAP2609 yields cleavage products of maximum 8 amino

residues in length (13, 33). Even though Cao's data showed that low molecular weight fraction of SDCM did not lose its resuscitative effect after treatment with digestive enzymes (13), there is no data available supporting that a peptide that small can have a resuscitative effect. Moreover, there were no bands detected on SDS-PAGE gel of the 10X concentrates of low molecular weight fractions of SDCM in 0-10kDa range, suggesting that peptides are not present in significant concentrations in the fraction of SDCM with resuscitative effect. Assays aimed to measure protein/peptide (Biuret and BCA assays) concentration based on peptide bond detection as well did not provide supportive data. Though based on the colorimetric data from both of the assays all of the fractions had significant amount of protein , both Biuret and BCA assays are susceptible to interfering agents such as ascorbic acids, lipids, cysteine, chelating agents, and agents with reducing potential (25, 78). Since other than ultrafiltration, samples were not purified and no significant bands were revealed on SDS- PAGE gels, high concentration of proteins suggested by BCA assay is most likely to be attributed to interference of other substances present in the fractions. Based on earlier findings and data obtained in the present study, it can be concluded that peptides are not likely to be responsible for the resuscitative properties of low molecular weight fraction of SDCM.

Analysis of the low molecular weight fraction of SDCM across its absorbance spectrum revealed a peak at 220nm that is characteristic for a large number of organic compounds, including lipids and fatty acids. Considering that only SDCM fractions from cultures that preserved their acid-fast properties were able to enhance the recovery of dormant MAP cells, it is reasonable to speculate that a link exists between resuscitation

and lipid metabolism in starvation-dormant MAP. A closer look at lipid composition of outer membrane of mycobacteria shows that the most abundant lipids are free mycolic acids (MA) and fatty acids (FA), triacylglicerides (TAGs), and glycopeptidolipids (GPLs) which include 2.06%, 2.54%, and 5.56% of dry cell mass (dcm), respectively (5). All of the above-mentioned lipid compounds are less than 2kDa in size; thus, they can be present in the low molecular weight fraction of SDCM.

It has been shown that starvation-dormant MAP cells indeed have a different cell wall mycolate composition with an increased proportion of more compact ketomycolates, which might decrease permeability and confer enhanced resistance to harsh environmental conditions and toxic agents (3). Zhang *et al.* explored the possibility of phospholipids serving as resuscitative factors for dormant mycobacteria. They provided data that the addition of phosphatidyl-L-serine, a precursor of phosphatydil ethanolamine and phosphatidyl choline, alone has a resuscitative and growth promoting effect. The resuscitative effect was abolished by treatment with phospholipase A2 and C (92). Glycopeptidolipids (GPLs) were reported to be involved in biofilm formation, which can enhance survival in nutrient-depleted conditions (9, 19). In the current study thin layer chromatography revealed the presence of glycolipids in low molecular weight fractions of SDCM derived from cultures that preserved acid-fastness, but not from cultures with mixed or non-acid-fast phenotypes. Both of the fractions with resuscitative effect had GPL bands that migrated similarly to phosphatidyl choline; however, one of the fractions also had a GPL with a different migration pattern. A glycolipid band was also observed in the low molecular fraction of ADCM, with migration pattern closer to phosphatidyl

ethanolamine. Since there has not been detected a precise pattern of GPL distribution among the fractions, it is unlikely that GPLs are responsible for the resuscitative properties of low molecular weight fraction of SDCM.

Interestingly, mycolic acid methyl ester (MAME) composition differed among the low molecular weight fractions derived from CM of starvation dormant MAP cells with different phenotypes. Different MAMEs have also been detected in fractions derived from ADCM. It is worth mentioning that MAMEs found in CM fractions differed from the ones extracted from MAP whole cell lysates, suggesting that they are not cell wall-associated and are most likely secreted by the bacteria.

The low molecular weight fraction of SDCM from acid-fast dormant MAP cells was able to promote resuscitation only at a higher dilution, which is consistent with the observation made by Ghimire (27). Shleeva *et al.* in their resuscitation study of dormant *M. smegmatis* and *Mtb* as well report that fatty acids were able to enhance bacterial growth only within the optimal concentration range, higher concentrations of FAs leading to cell membrane disruption and damage. In their study FAs mostly likely served as signal molecules that, when sensed by adenylyl cyclase, led to increase of cAMP which in turn upregulated expression of Rpf proteins by an as yet unknown pathway (70). Data obtained from the present study can be correlated with the observations made by Shleeva and her group. If mycolic acids are involved in resuscitation process, it is most likely a combination of a specific type of MA and its optimal concentration that have resuscitative potential. Based on the band intensity of detected MAMEs and using BCA assay data as indirect method of lipid concentration measurement, the samples with

highest concentration of MAMEs had inhibitory effect on MAP growth. Fractions that had resuscitative effect had comparable MAME concentration to non-resuscitative fractions; however, a different migration pattern of MAMEs was characteristic.

There were a few limitations in the conducted study that might have affected the outcomes. First of them was the appearance of growth "spikes" in some of the optical density reads during resuscitative assays that did not continue in the following reading. The nature of "spikes" is unlikely related to the actual bacterial growth, but rather is caused by condensation or mechanical issues; however, it did generate larger standard deviation within the sample and complicated statistical analysis of the acquired data.

Secondly, the experimental setup might not have been identical for all the samples. Due to the tendency of MAP cells to clump, it is difficult to inoculate wells evenly. Hence, reduced number of positive wells in certain fractions interpreted as lack of resuscitative activity might have been caused by suboptimal inoculation of other wells. Similar issues have been encountered by Cao (13) and protocol revision and/or modification need to be done in order to yield more reliable data.

Another drawback of the study was the potential loss of mycolic acids and lipids during lipid extraction step for thin layer chromatography, which might have resulted in underrepresentation of lipid diversity and concentration in the samples. Large quantities of conditioned media are needed to correct this issue; however, due to time-consuming process of acquiring conditioned media from dormant cells, larger facility is needed.

Finally, even though presence of a significant amount of peptides/ amino acid polymers in the low molecular weight fraction of SDCM is unlikely, purification of samples from putative interfering agents in order to increase specificity of BCA assay is beneficial.

Lipid involvement in resuscitation of MAP is a reasonable hypothesis for further investigation taking into consideration the results of the present study and supportive data from other research groups (70, 92). However, prior to considering it a primary driver of resuscitation induced by addition of low molecular weight fraction of SDCM to the growth medium, resuscitative role of other macromolecules should be assessed first. Shleeva et al. demonstrated that increase in cAMP levels on its own had a growth-promoting effect on *M. smegmatis* (70). It is a fundamental knowledge that nucleotides have an indispensable role in metabolism and cell communication often serving as second messengers and/or energy blocks. Hence, nucleotides and cyclic nucleotides can be involved in resuscitation of dormant cells and need to be investigated.

Another class of macromolecules that deserves attention is carbohydrates. Carbohydrates are linked to cell signaling, serve as receptors and energy source. Several studies demonstrated involvement of carbohydrate metabolism into dormancy and resuscitation of mycobacteria. It has been shown that dormant *M. smegmatis* has increased accumulation of free trehalose accumulation (64% of total organic substances) compared to early stationary phase (15% of total organic substances) (71). Dormant cells with higher free trehalose amount also survived much better compared to dormant cells with lower trehalose levels. Trehalose levels diminished during early resuscitation phase

suggesting their importance for the recovery of dormant cells (71). It is possible that besides just storing trehalose dormant mycobacteria can also secrete trehalose or other carbohydrate. Carbohydrates as well as nucleotides are potential candidates for the role of resuscitative factor in low molecular weight fraction of SDCM. A closer look at carbohydrate composition of the SDCM fractions might move some stumbling blocks in the understanding the mechanism of resuscitation of MAP or provide some supportive data to refute their involvement in the recovery of dormant cells.

CONCLUSION

Dormancy has an effect on the lipid metabolism of MAP cells, particularly mycolic acids, that can be reflected in three phenotypes: dormant cells that preserve acid-fastness, non- acid fast dormant cells, and intermediate mixed phenotype.

Growth-promoting effect of conditioned media derived from starvation-dormant cells on anaerobically-dormant MAP cells suggests presence of resuscitative factors. Earlier studies defined them as molecules smaller than 5kDa in size, heat- and protease-(trypsin and thermolysin) stable, refuting the hypotheses of growth-promoting factors belonging to Rpf family of protein or being MAP2609, a homolog of Rv1174c found in *Mtb.* The absence of the peak at 280nm in absorbance spectrum and inconclusive Biuret assay and BCA assays results supported the hypothesis that resuscitative factors were not proteinaceous in nature. SDS-PAGE gel electrophoresis of 10X concentrates of the low molecular weight fractions of SDCM with further staining by Coomassie Blue stain and silver nitrate did not detect bands of 5kDa and smaller as well.

Resuscitative effect was observed only from the low molecular weight fractions derived from cultures with preserved acid-fast properties, suggesting a link to lipid metabolism. Resuscitative effect was also observed only in higher dilutions of respective fractions, suggesting toxicity or inhibitory effect of factors found in CM at a higher concentration.

Thin layer chromatography for glycolipids detected glycolipids in fractions of SDCM from acid-fast fractions and from fraction derived from anaerobically-dormant

cells, but no specific trend in glycolipid distribution was observed decreasing the likelihood of the role of glycolipids in resuscitation from the dormant state.

TLC detecting MAMEs and FAMEs revealed different subtypes of mycolic acids depending on the phenotype of the culture the fraction was derived from. MAMEs detected in the fractions of CM differed from the ones extracted from MAP whole cell lysates, suggesting that they are not cell wall-associated and are most likely secreted by the bacteria. If mycolic acids are indeed involved in resuscitation of MAP from the dormant state, it is most likely a combination of a specific type of MA and its optimal concentration that have resuscitative potential.

The present study, however, had a few limitations. Unexpected spikes of optical density were detected in many wells during resuscitative assay, which tended to disappear suddenly, suggesting that they were not related to the actual MAP growth. The tendency of MAP to clump also could have affected the ability to inoculate the wells with equal amounts of bacteria. Both of the issues might have had an effect on statistical analysis of the data and were responsible for high standard deviations.

Complicated extraction protocols for TLC samples could have resulted in significant loss of the sample and hence incomplete data. However, significantly larger amounts of bacteria have to be grown to overcome this problem, which is time-consuming and requires a larger facility.

Finally, in order to provide more evidence that resuscitative factors are not based of amino acids, samples for the BCA assay should be purified from the potential

interfering agents. Other important macromolecules to consider for investigation are nucleotides, cyclic nucleotides and carbohydrates.

The present study yielded data that is suggesting that lipids, particularly mycolic acids, might have resuscitative properties found in SDCM. It is plausible to speculate on lipid involvement based on size, peaks in absorbance spectrum, disappearance of resuscitative effect at higher concentrations of SDCM, and TLC data. Nevertheless, further work is required in order to test this hypothesis. Extraction of mycolic acids from TLC plates, purification, and analysis with mass spectrometry could provide valuable data. Preparative HPLC and isolation of lipid components from the low molecular fraction of SDCM can be used for direct testing of resuscitative effect using a modified protocol addressing the issues mentioned above. If lipids indeed are the ones responsible for resuscitative effect of SDCM, more questions arise regarding the pathway they act on. Do they directly promote growth and recovery from the dormant state or are they a part of a cascade? If part of the cascade, which molecule is the key component of it and what is the optimal dose for resuscitative effect?

If identified, resuscitative factors found in SDCM can be bioengineered and supplemented to the growth media used for diagnostic fecal culture resulting in a higher sensitivity of the method. Therefore, it is hoped that the findings of the present study contributed to the improvement of diagnosis of Johne’s disease and, sequentially, its better management. This, in turn, will lessen financial losses associated with JD, improve the quality of dairy products, and possibly improve the management of autoimmune disorders associated with MAP infection in human population.

REFERENCES

1. **Alnimr, AM**. 2015. Dormancy models for Mycobacterium tuberculosis: A minireview. Braz J Microbiol 46(3):641-647.
2. **Alphalyse.** 2001. Protocol for silver staining of gels. Alphalyse, Palo Alto, CA.
3. **Archuleta RJ, Hoppes PY, Primm TP.** 2005. *Mycobacterium avium* enters a state of metabolic dormancy in response to starvation. Tuberculosis 85:147-158.
4. **Bannantine JP. Talaat AM.** 2015. Controlling Johne's disease: vaccination is the way forward. Front Cell Infect Microbiol 5:2.
5. **Bansal-Mutalik R, Nikaido H.** 2014. Mycobacterial outer membrane is a lipid bilayer and the inner membrane is unusually rich in diacyl phosphatidylinositol dimannosides. PNAS 111(13):4958-4963.
6. **Begg DJ, de Silva K, Carter N, Plain KM, Purdie A, Whittington RJ.** 2011. Does a Th1 over Th2 dominancy really exist in the early stages of *Mycobacterium avium* subspecies *paratuberculosis* infections? Immunobiology 216:840-846.
7. **Beran V, Havelkova M, Kaustova J, Dvorska L, Pavlik I.** 2006. Cell wall deficient forms of mycobacteria: a review. Veterinarni Medicina 51(7):365-389.
8. **Betts JC, Lukey PT, Robb LC, McAdam RA, Duncan K.** 2002. Evaluation of nutrient starvation model of *Mycobacterium tuberculosis* persistence by gene and protein expression profiling. Mol Microbiol 43(3):717-731.
9. **Beumer A, King D, Donohue M, Mistry J, Covert T, Pfaller S.** 2010. Detection of *Mycobacterium avium* subsp. *paratuberculosis* in drinking water and biofilms by quantitative PCR. Appl Environ Microbiol 76(21):7367-7370.

10. **Bio-Rad.** 2011. Mini-PROTEAN® precast gels. Instruction manual and application guide. Bulletin 1658100. Bio-Rad, Hercules, CA.
11. **Bo M, Niegowska M, Arru G, Sechi E, Mariotto S, Mancinelli C, Farinazzo A, Alberti D, Gajofatto A, Ferrari S, Capra R, Monaco S, Sechi G, Sechi LA.** 2018. *Mycobacterium avium* subscpecies *paratuberculosis* and myelin basic protein specific epitopes are highly recognized by sera from patients with Neuromyelitis optica spectrum disorder. J Neuroimmunol 318:97-102.
12. **Bull TJ, Gilbert SC, Sridhar S, Linedale R, Dierkes N, Sidi-Boumedine K, Hermon-Taylor J.** 2007. A novel multi-antigen virally vectored vaccine against *Mycobacterium avium* subsp. *paratuberculosis.* PLoS One 2:e1229.
13. **Cao TM**. 2012. MS Thesis. Minnesota State University Mankato, Mankato, MN. Identification of factors that promote the growth of dormant *Mycobacterium avium* subsp. *paratuberculosis.*
14. **Chacon O, Bermudez LE, Barletta RG.** 2004. Johne's disease, inflammatory bowel disease, and *Mycobacterium paratuberculosis.* Annu Rev Microbiol 58:329-363.
15. **Chandramouli V, Venkitasubramanian TA.** 1974. Effect of age on the lipids of Mycobacteria. Indian J Chest Dis 16:199-207.
16. **Chengalroyen MD, Beukes GM, Gordhan BG, Streicher EM, Churchyard G, Hafner R, Warren R, Otwombe K, Martinson N, Kana BD.** 2016. Detection and quantification of differentially culturable tubercle bacteria in sputum from patients with tuberculosis. Am J Respir Crit Care Med 194(12):1532-1540.

17. **Chiodini RJ, Van Kruiningen HJ, Merkal RS.** 1984. Ruminant paratuberculosis (Johne's disease): the current status and future prospects. Cornell Vet 74(2):218-262.

18. **Cocito C, Gilot P, Coene M, De Kesel M, Poupart P, Vannuffel P.** 1994. Paratuberculosis. Clin Microbiol Rev 7(3):328-245.

19. **Dhouib R, Laval F, Carrière F, Daffé M, Canaan S.** 2010. A monoacylglycerol lipase from *Mycobacterium smegmatis* involved in bacterial cell interaction. J Bacteriol 192(18):4776-4785.

20. **Dupont CM, Kremer L.** 2014. Extraction and purification of mycobacterial mycolic acids. Bio Protoc 4(20):e1265.

21. **Elliot GN, Hough RL, Avery LM, Maltin CA, Campbell CD.** 2014. Environmental risk factors in the incidence of Johne's disease. Crit Rev Microbiol 41:4: 488-507.

22. **Faisal SM, Chen JW, Yan F, Chen TT, Useh NM, Yan W, Guo S, Wang SJ, Glaser AL, McDonough SP, Singh B, Davis WC, Akey BL, Chang YF.** 2013. Evaluation of *Mycobacterium avium* subsp. *paratuberculosis leuD* mutant as a vaccine candidate against challenge in a caprine model. Clin Vaccine Immunol 20(4):572-581.

23. **Folch J, Lees M, Stanley GHS**. 1957. A simple method for the isolation and purification of total lipids from animal tissue. J Biol Chem 226:497-509.

24. **Gao A, Mutharia L, Chen S, Rahn K, Odumeru J.** 2002. Effect of pasteurization on survival of *Mycobacterium paratuberculosis* in milk. J Dairy

Sci 85(12):3198-3205.

25. **G-Biosciences.** 2014. Biuret protein assay. Teacher's handbook (Cat. #BE-402B). G-Biosciences, St.Louis, MO.
26. **Geraghty T, Graham DA, Mullowney P, More SJ.** 2014. A review of bovine Johne's disease control activities in 6 endemically infected countries. Prev Vet Med 116:1-11.
27. **Ghimire E.** 2011. MS Thesis. Minnesota State University Mankato, Mankato, MN. Effect of conditioned medium and cell lysate on the recovery of dormant *Mycobacterium avium* subsp. *paratuberculosis.*
28. **Ghosh P, Shippy DC, Talaat AM.** 2015. Superior protection elicited by live-attenuated vaccines in the murine model of paratuberculosis. Vaccine 33:7262-7270.
29. **Ghosh P, Steinberg H, Talaat AM.** 2014. Virulence and immunity orchestrated by the global gene regulator sigL in *Mycobacterium avium* subsp. *paratuberculosis.* Infect Immun 82:2066-2075.
30. **Grant IR, Kirk RB, Hitchings E.** 2003. Comparative evaluation of the MGIT and BACTEC culture systems for the recovery of *Mycobacterium avium* subsp. *paratuberculosis* from milk. J Appl Microbiol 95:196-201.
31. **Gumber S, Taylor DL, Whittington RJ.** 2009. Evaluation of the immunogenicity of recombinant stress-associated proteins during *Mycobacterium avium* subsp. *paratuberculosis* infection: implications for pathogenesis and diagnosis. Vet Microbiol 137:290-296.

32. **Harris NB, Barletta RG.** 2001. *Mycobacterium avium* subsp. *paratuberculosis* in veterinary medicine. Clin Microbiol Rev 14(3):489-512.

33. **Hedlund DD.** 2010. MS Thesis. Minnesota State University Mankato, Mankato, MN. Bioinformatics and sequence analysis of four resuscitation promoting factor (Rpf) gene homologues in *Mycobacterium avium* subsp. *paratuberculosis* (Mpt), and expression of the putative Mpt Rpfb in *Escherichia coli.*

34. **Huygen K.** 2006. DNA vaccines against mycobacterial diseases. Future Microbiol 1:63-73.

35. **Inderlied CB, Kemper CA, Bermudez LEM.** 1993. The *Mycobacterium avium* complex. Clin Microbiol Rev 6(3):266-310.

36. **Iona E, Pardini M, Mustazzolu A, Piccaro G, Nisini R, Fattorini L, Giannoni F.** 2016. *Mycobacterium tuberculosis* gene expression at different stages of hypoxia-induced dormancy and upon resuscitation. J Microbiol 54(8):565-572.

37. **Irenge LM, Walravens K, Govaerts M, Godfroid J, Rosseels V, Huygen K, Gala JL.** 2009. Development and validation of a triplex real-time PCR for rapid detection and specific identification of *M. avium* sub sp. *paratuberculosis* in faecal samples. Vet Mictobiol 136(1-2):166-172.

38. **Koets A, Hoek A, Langelaar M, Overdijk M, Santema W, Franken P, van Eden W, Rutten V.** 2006. Mycobacterial 70kD heat-shock protein is an effective subunit vaccine against bovine paratuberculosis. 24:2550-2559.

39. **Kohler H, Gyra H, Zimmer K, Dräger KG, Burkert B, Lemser B, Hausleithner D, Cubler K, Klawonn W, Hess RG.** 2001. Immune reactions in

cattle after immunization with *Mycobacterium paratuberculosis* vaccine and implications for the diagnosis of *M. paratuberculosis* and *M. bovis* infections. J Vet Med B Infect Dis Vet Public Health 48(3):185-195.

40. **Kuehnel MP, Goethe R, Habermann A, Mueller E, Rohde M, Griffiths G, Valentin-Weigand P.** 2001. Characterization of the intracellular survival of *Mycobacterium avium* ssp. *paratuberculosis*: phagosomal pH and fusogenicity in J774 macrophages compared with other mycobacteria.
41. **Lamont EA, Bannantine JP, Armién A, Ariyakumar DS, Sreevatsan S**. 2012. Identification and characterization of a spore-like morphotype in chronically starved *Mycobacterium avium* subsp. *paratuberculosis* cultures. PLoS One 7(1):e30648.
42. **Leite CQF, Oliveira de Souza CW, de Andrade Leite SR.** 1998. Identification of mycobacteria by thin layer chromatographic analysis of mycolic acids and conventional biochemical method: four years of experience. Mem Inst Oswaldo Cruz 93(6):801-805.
43. **Li L, Bannantine JP, Zhang Q, Amonsin A, May BJ, Alt D, Banerji N, Kanjilal S, Kapur V.** 2005. The complete genome sequence of *Mycobacterium avium* subspecies *paratuberculosis.* PNAS 102(35):12344-12349.
44. **Lipworth S, Hammond RJH, Baron VO, Hu Y, Coates A, Gillespie SH.** 2016. Defining dormancy in mycobacterial disease. Tuberculosis 99:131-142.
45. **Loebel RO, Shorr E, Richardson HB.** 1933. The influence of adverse conditions upon the respiratory metabolism and growth of human tubercle bacilli.

J Bacteriol 26(2):167-200.

46. **Lombard JE, Gardner IA, Jafarzadeh SR, Fossler CP, Harris B, Capsel RT, Wagner BA, Johnson WO.** 2013. Herd-level prevalence of *Mycobacterium avium* subsp. *paratuberculosis* infection in United States dairy herds in 2007. Prev Vet Med 108(2-3):234-238.
47. **Losinger WC.** 2005. Economic impact of reduced milk production associated with Johne's disease on diary operation on the USA. J Dairy Res 72:425-432.
48. **Manning EJB, Collins MT.** 2001. *Mycobacterium avium* subsp. *paratuberculosis:* pathogen, pathogenesis and diagnosis. Rev sci tech Off int Epiz 20(1):133-150.
49. **McGillivray A, Golden NA, Kaushal D.** 2015. The *Mycobacterium tuberculosis* Clp gene regulator is required for *in vitro* reactivation from hypoxia-induced dormancy. J Biol Chem 290(4):2351-2367.
50. **McNees AL, Markesich D, Zayyani NR, Graham DY.** 2015. *Mycobacterium paratuberculosis* as a cause of Crohn's disease. Expert Rev Gastroenterol Hepatol 9(12): 1523–1534.
51. **Minnikin DE, Hutchinson IG, Caldicott AB.** 1980. Thin-layer chromatography of methanolysates of mycolic acid-containing bacteria. J Chromatogr 188:221-233.
52. **Molecular Probes.** 2004. LIVE/DEAD® BacLight™ bacterial viability kits.Molecular Probes, Eugene, OR.
53. **Momotani E, Whipple DL, Thiermann AB, Cheville NF.** 1988. Role of M cells

and macrophages in the entrance of *Mycobacterium paratuberculosis* into domes of ileal Peyer's patches in calves. Vet Pathol 25:131-137.

54. **Mortier RA, Barkema HW, Wilson TA, Sajobi TT, Wolf R, De Buck J**. 2014. Dose-dependent interferon-gamma release in dairy calves experimentally infected with *Mycobacterium avium* subsp. *paratuberculosis*. Vet Immunol Immunopathol 161:205-210.
55. **Mukamolova GV, Murzin AG, Salina EG, Demina GR, Kell DB, Kaprelyants AS, Young M.** 2006. Muralytic activity of *Micrococcus luteus* Rpf and its relationship to physiological activity in promoting bacterial growth. Mol Microbiol 59:84-98.
56. **Nikitushkin VD, Demina GR, Kaprelyants AS.** 2016. Rpf proteins are the factors of reactivation of the dormant forms of *Actinobacteria.* Biochemistry (Mosc) 81(13):1719-1732.
57. **O'Brien R, Hughes A, Liggett S, Griffin F.** 2013. Composite testing for ante-mortem diagnosis of Johne's disease in farmed New Zealand deer: correlations between bacteriological culture, histopathology, serological reactivity and faecal shedding as determined by quantitative PCR. BMC Vet Res 9:72.
58. **Olsen I, Reitan LJ, Holstad G, Wiker HG.** 2000. Alkyl hydroperoxide reductases C and D are major antigens constitutively expressed by *Mycobacterium avium* subsp. *paratuberculosis.* Infect Immunol 68:801-808.
59. **Ott SL, Wells SJ, Wagner BA.** 1999. Herd-level economic losses associated with Johne's disease on US dairy operations. Prev Vet Med 40:179-192.

60. **Paolicchi F, Cirone K, Morsella C, Gioffré A.** 2012. First isolation of *Mycobacterium avium* subsp. *paratuberculosis* from commercial pasteurized milk in Argentina. Braz J Microbiol 43(3):1034-1037.

61. **Park H-T, Shin M-K, Park H-E, Cho Y-I, Yoo HS.** 2016. PCR-based detection of Mycobacterium avium subsp. paratuberculosis infection in cattle in South Korea using fecal samples. J Vet Med Sci 78(9):1537-1540.

62. **Park H-T, Yoo HS.** 2016. Development of vaccines to *Mycobacterium avium* subsp. *paratuberculosis* infection. Clin Exp Vaccine Res 5:108-116.

63. **Reading NC, Sperandio V.** 2006. Quorum sensing: the many languages of bacteria. FEMS Microbiol Lett 254:1-11.

64. **Rosseels V, Marché S, Roupie V, Govaerts M, Godfroid J, Walravens K, Huygen K.** 2006. Members of the 30- to 32-kilodalton mycolyl transferase family (Ag85) from culture filtrate of *Mycobacterium avium* subsp. *paratuberculosis* are immunodominant Th1-type antigens recognized early upon infection in mice and cattle. Infect Immun 74:202-212.

65. **Santema W, Hensen S, Rutten V, Koets** A. 2009. Heat shock protein 70 subunit vaccination against bovine paratuberculosis does not interfere with current immunodiagnostic assays for bovine tuberculosis. 27:2312-2319.

66. **Schönenbrücher H, Abdulmawjood A, Failing K, Bülte M**. 2008. New triplex real-time PCR assay for detection of *Mycobacterium avium* subsp. *paratuberculosis* in bovine feces. Appl Environ Microbiol 74(9):2751-2758.

67. **Schubert OT, Ludwig C, Kogadeeva M, Zimmermann M, Rosenberg G,**

Gengenbacher M, Gillet LC, Collins BC, Röst HL, Kaufmann SH, Sauer U, Aebersold R. 2015. Absolute proteome composition and dynamics during dormancy and resuscitation of *Mycobacterium tuberculosis*. Cell Host Microbe 18(1):96-108.

68. **Sergeant ES, Whittington RJ, More SJ.** 2002. Sensitivity and specificity of pooled fecal culture and serology as flock-screening tests for detection of ovine paratuberculosis in Australia. Prev Vet Med 52:199-211.
69. **Shinnick TM, Good RC.** 1994. Mycobacterial taxonomy. Eur J Clin Microbiol Infect Dis 13(11):884-901.
70. **Shleeva M, Goncharenko A, Kudykina Y, Young D, Young M, Kaprelyants A.** 2013. Cyclic AMP-dependent resuscitation of dormant mycobacteria by exogenous free fatty acids. PLoS One 8(12):e82914.
71. **Shleeva MO, Trutneva KA, Demina GR, Zinin AI, Sorokoumova GM, Laptinskaya PK, Shumkova ES, Kaprelyants AS.** 2017. Free trehalose accumulation in dormant *Mycobacterium smegmatis* cells and its breakdown in early resuscitation phase. Front Microbiol 8:524.
72. **Singh P**, **Sinha R, Tandon R, Tyagi G, Khatri P, Chandra Shekhar Reddy L, Saini NK, Pathak R, Varma-Basil M, Prasad AK, Bose M.** 2014. Revising a protocol for extraction of mycobacterial lipids. Int J Mycobacteriol 3:168-172.
73. **Slana I, Liapi M, Moravkova M, Kralova A, Pavlik I.** 2009. *Mycobacterium avium* subsp. *paratuberculosis*in cow bulk tank milk in Cyprus detected by culture and quantitative IS*900* and F*57* real-time PCR. Pre Vet Med 89:223-226.

74. **Stevenson, K.** 2015. Genetic diversity of *Mycobacterium avium* subspecies *paratuberculosis* and the influence of strain type on infection and pathogenesis: a review. Vet Res 46:64.

75. **Strommenger B, Stevenson K, Gerlach GF.** 2001. Isolation and diagnostic potential of IS*Mav2*, a novel insertion sequence-like element from *Mycobacterium avium* subsp. *paratuberculosis.* FEMS Microbiol Lett 196:31-37.

76. **Sweeney RW, Jones DE, Habecker P, Scott P.** 1998. Interferon-gamma and interleukin 4 gene expression in cows infected with *Mycobacterium paratuberculosis.* Am J Vet Res 59:842-847.

77. **Taneja NK, Tyagi JS.** 2007. Resazurin reduction assay for screening of anti-tubercular compounds against dormant and actively growing *Mycobacterium tuberculosis, Mycobacterium bovis* BCG and *Mycobacterium smegmatis.* J Antimicrob Chemother 60:288-293.

78. **Thermo Scientific.** 2007. User guide: Pierce BCA protein assay kit (MAN0011430 Rev.A). Thermo Scientific, Rockford, IL.

79. **Totani T, Nishiuchi Y, Tateishi Y, Yoshida Y, Kitanaka H, Niki M, Kaneko Y, Matsumoto S.** 2017. Effects of nutritional and ambient oxygen condition on biofilm formation in *Mycobacterium avium* subsp. *hominissuis* via altered glycolipid expression. Sci Rep 7:41775.

80. United States Department of Agriculture. National Animal Health Monitoring System Dairy 1996 brochure.

81. United States Department of Agriculture. National Animal Health Monitoring

System Dairy 2007 brochure.

82. **Veatch AV, Kaushal D.** 2018. Opening Pandora's box: mechanisms of *Mycobacterium tuberculosis* resuscitation. Trends Microbiol 26(2):145-157.

83. **Vorbeck ML**, **Marinetti GV.** 1965. Separation of glycosyl digycerides from phosphatides using silicic acid column chromatography. J Lipid Res 6:3-6.

84. **Voskuil MI, Schnappinger D, Visconti KC, Harrell MI, Dolganov GM, Sherman DR, Schoolnik GK.** 2003. Inhibition of respiration by nitric oxide induces a *Mycobacterium tuberculosis* dormancy program. J Exp Med 198(5):705-713.

85. **Wayne LG, Hayes LG.** 1996. An *in vitro* model for sequential study of shiftdown of *Mycobacterium tuberculosis* through two stages of nonreplicating persistence. Infect Immun 64:2062-2069.

86. **Wayne LG, Sohaskey CD.** 2001. Nonreplicating persistence of *Mycobacterium tuberculosis*. Annu Rev Microbiol 55:139-163.

87. **Wayne LG, Sramek HA.** 1994. Metronidazole is bactericidal to dormant cells of *Mycobacterium tuberculosis.* Antimicrob Agents Chemother 38(9):2054-2058.

88. **Whitlock RH, Wells SJ, Sweeney RW, Van Tiem J**. 2000. ELISA and fecal culture for paratuberculosis (Johne's disease): sensitivity and specificity of each method. Vet Microbiol 77:387-398.

89. **Whittington RJ, Jeff Marshall D, Nicholls PJ, Marsh IB, Reddacliff LA.** 2004. Survival and dormancy of *Mycobacterium avium* subsp. *paratuberculosis* in the environment. Appl Environ Microbiol 70(5):2989-3004.

90. Whittington RJ, Marsh I, McAllister S, Turner MJ, Marshall DJ, Fraser CA. 1990. Evaluation of modified BACTEC 12B radiometric medium and solid media for culture of *Mycobacterium avium* subsp. *paratuberculosis* from sheep. J Clin Microbiol 37:1077-1083.

91. Windsor PA, Eppleston J, Dhand NK, Whittington RJ. 2014. Effectiveness of Gudair vaccine for the control of ovine Johne's disease in flocks vaccinating for at least 5 years. Aust Vet J 92:263-268.

92. Zhang Y, Yang Y, Woods A, Cotter RJ, Sun Z. 2001. Resuscitation of dormant Mycobacterium tuberculosis by phospholipids or specific peptides. Biochem Biophys Res Commun 284:542-547.

93. Zhu W, Plikaytis BBB, Shinnick TM. 2003. Resuscitation factors from mycobacteria: homologs of *Micrococcus luteus* proteins. Tuberculosis 83:261-269.

APPENDIX

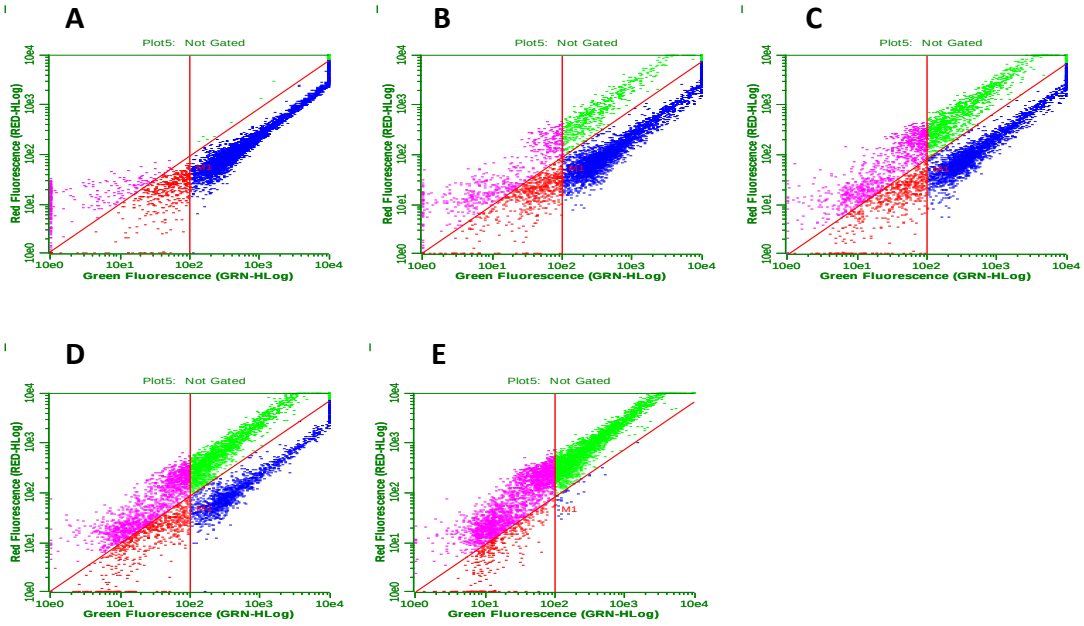

A1. Optimization of viability assay using flow cytometry. Log green fluorescence vs. log red fluorescence for MAP culture suspensions with 100%, 75%, 50%, 25%, and 0% viable cells mixed with SYTO9 and PI at equal proportions shown in panels **A, B, C, D, E,** respectively. Blue depicts viable cells stained with SYTO9 only. Green depicts dead cells stained with PI and SYTO9.

Table A1. Percentage of acquired by flow cytometry live cells compared to predicted values.

Predicted Live Cells, %	Acquired Live Cells, %			
	Sample 1	Sample 2	Sample 3	Sample 4
100	67.68	80.96	81.2	83.44
75	53.11	59.34	63.32	66.38
50	36.25	41.06	41.62	49.04
25	16.61	19.3	22.18	27.02
0	0.83	1.46	2.26	0.68

Percentage of viable cells in each suspension of samples 1, 2, 3, 4 mixed with equal proportions of SYTO9 and PI. Data acquired from flow cytometry log green fluorescence vs. log red fluorescence plots from experiment set up described in figure A1 repeated in quadruplicate.

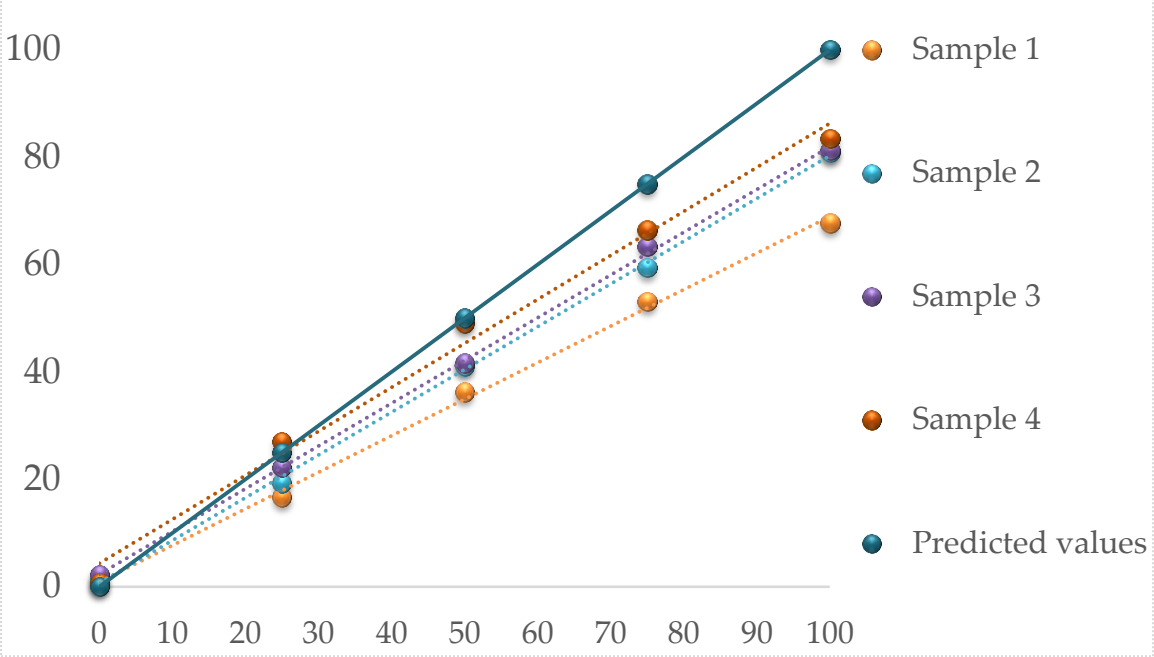

A2. Generation of standard curve and equation of the line for cell viability assessment via flow cytometry. Scatter plot of values of viable cells in a suspension (%) acquired via flow cytometry for each suspension of samples 1, 2, 3, 4 plotted against predicted values. Dotted lines represent linear trend lines for each data set. Solid line represents trend line for predicted values.

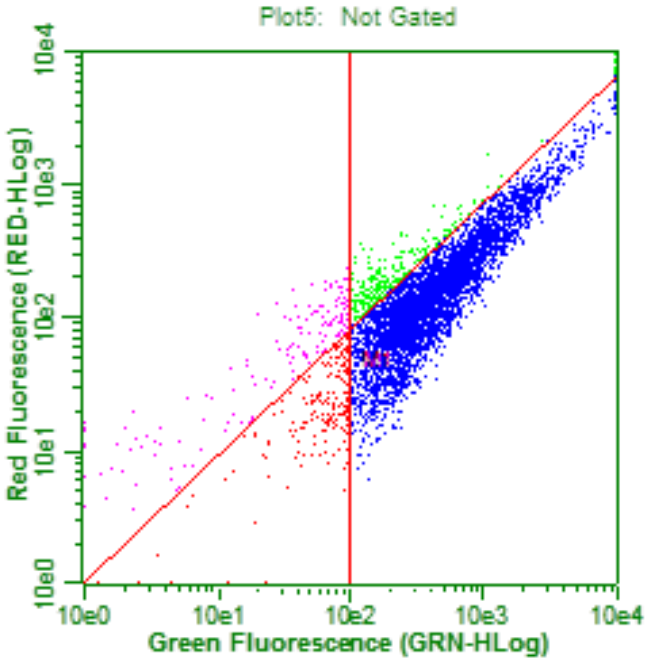

A3. Viability assay of starvation-dormant MAP cells. Blue cells represent viable cells, green – dead cells, red and pink – understained cells.

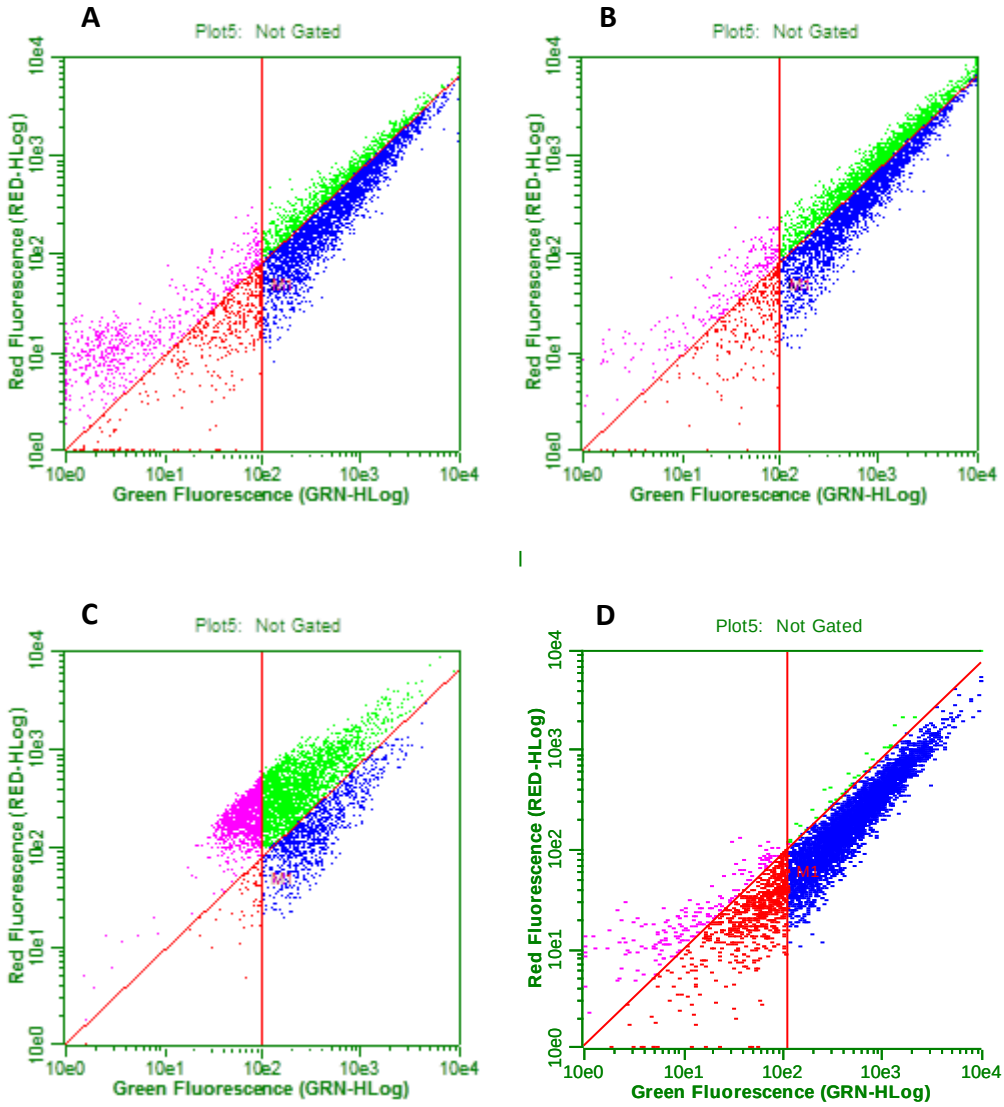

A4. Viability assay of anaerobically-dormant MAP cells. Cells were stained with SYTO9:PI mixed in equal proportions. Blue cells represent viable cells, green – dead cells, red and pink – understained cells. Panels A, B, and C represent one-year-old anaerobically dormant cultures, panel D represents three-months-old anaerobically dormant culture. **A**. Viable cells – 58.79%. **B.** Viable cells – 54.29%. **C**. Viable cells – 22.54%. **D**. Viable cells – 80.52%.

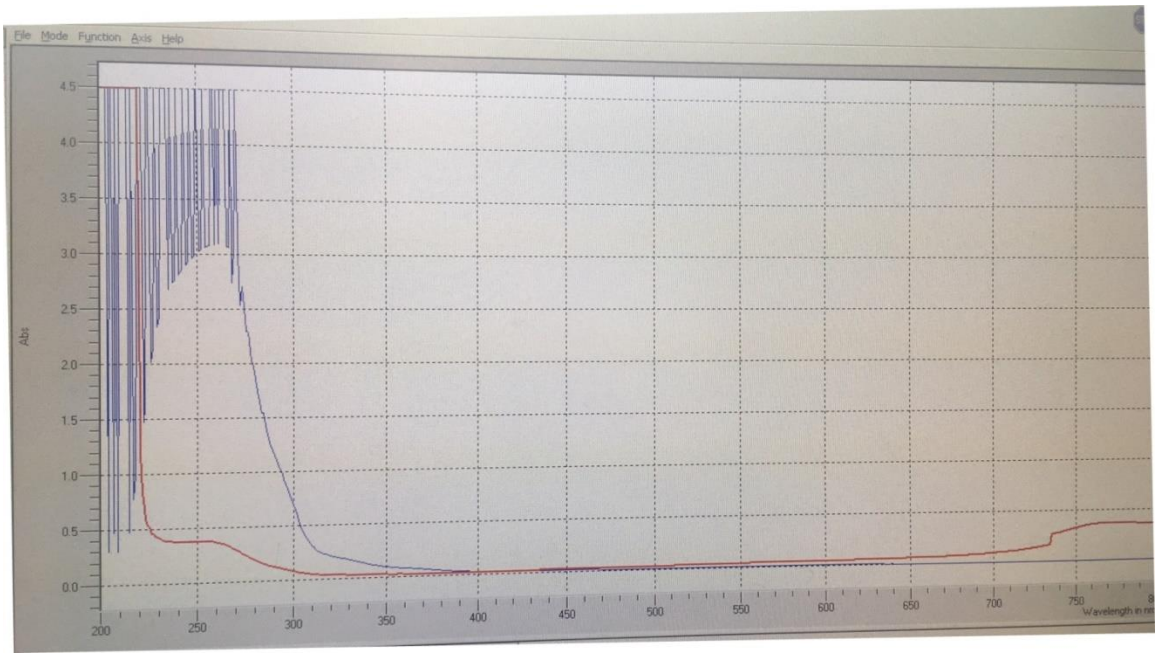

A5. Absorbance spectrum of the low molecular weight fraction of SDCM. Low molecular weight fraction of M7H9C growth medium supplemented with OADC was used as to blank spectrophotometer. One hundred microliters of the low molecular weight fraction of SDCM was screened across absorbance spectrum generating blue line. .One hundred microliters of diluted 1:10 low molecular weight fraction of SDCM was screened across absorbance spectrum generating red line.

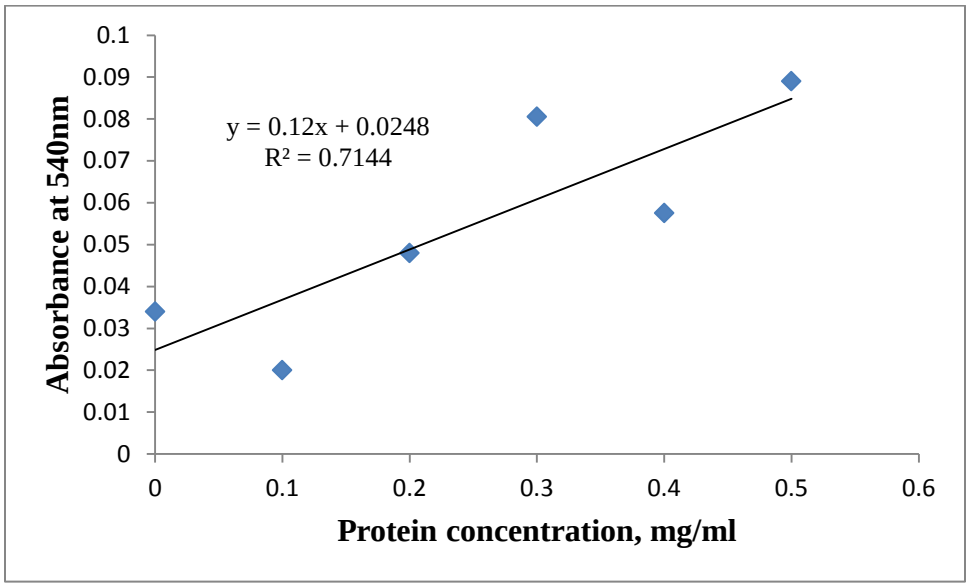

A6. Standard curve and equation of the line generated for Biuret assay. Duplicates of solutions of bovine serum albumin concentrations ranging from 0 to 0.5 mg/ml and Biuret reagent were prepared and incubated at room temperature for 20 minutes. Absorbance at 540nm was measured by spectrophotometer.

Table A2. Protein concentration in low molecular weight fractions of SDCM and ADCM determined by Biuret assay.

Sample #	Absorbance, 540nm	[Protein], mg/ml
T1	0.047	0.19
T2	0.053	0.24
T3	0.031	0.05
T4	0.062	0.31
T5	0.049	0.20
T6	0.056	0.26
T7	0.041	0.14
ADCM 12	0.043	0.15
ADCM 3	0.028	0.03

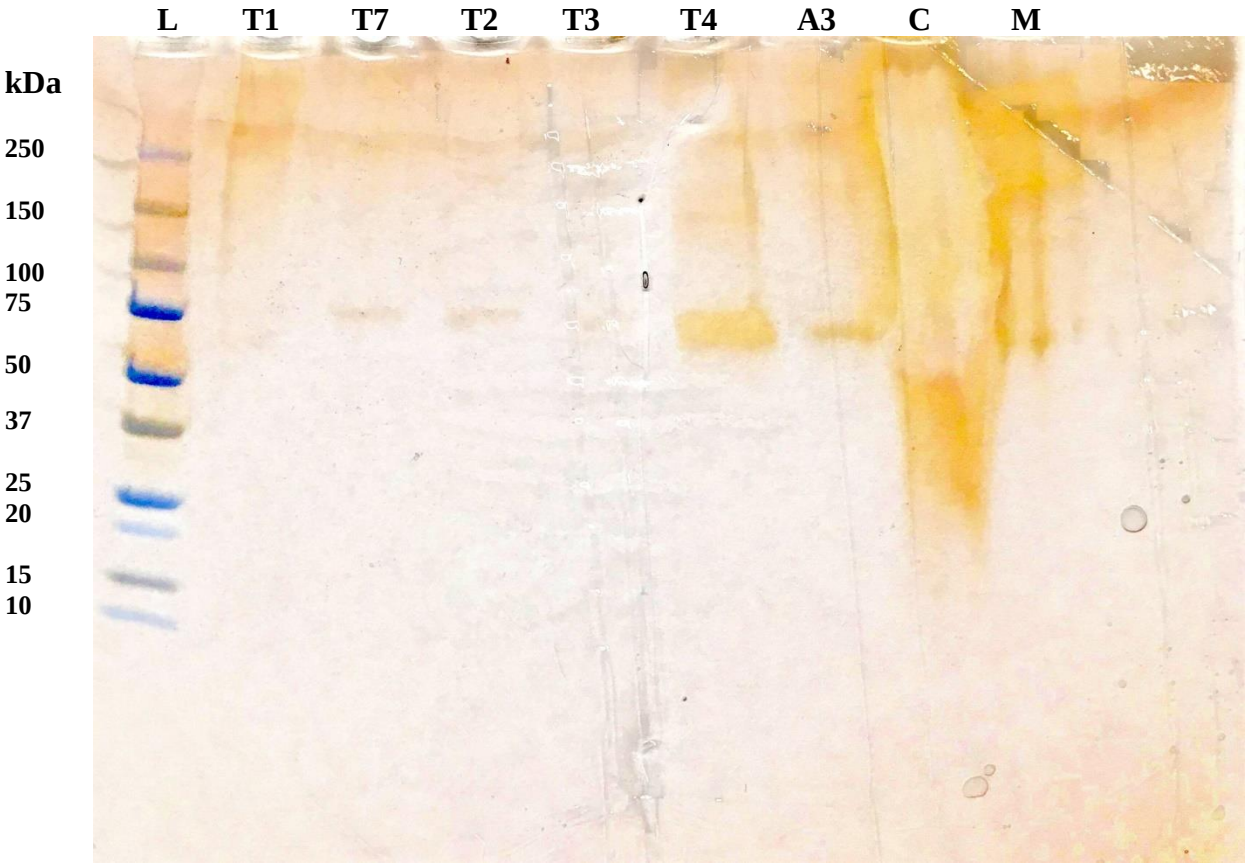

A7. Silver staining of SDS-PAGE gel with 10X concentrates of low molecular weight fractions of SDCM, ADCM, M7H9C growth media, and high molecular weight fraction of SDCM. Low molecular weight fractions of SDCM from T1, T2, T3, T4, T7, of ADCM from one-year-old cultures, and M7H9C growth media were lyophilized and resuspended in smaller volume in order to generate 10X concentrates. The samples were loaded on SDS-PAGE gels using Orange G loading dye. The samples were stained with silver nitrate in order to reveal proteins. **L** – protein standard ladder; **T1, T2, T3, T4, T7** – low molecular weight fractions of SDCM; **A3** - low molecular weight fractions of anaerobically-dormant conditioned media from three-month-old culture; **C** – high molecular weight fraction of SDCM containing molecules above 5kDa in size; **M** - low molecular weight fractions of M7H9C growth medium supplemented with OADC.

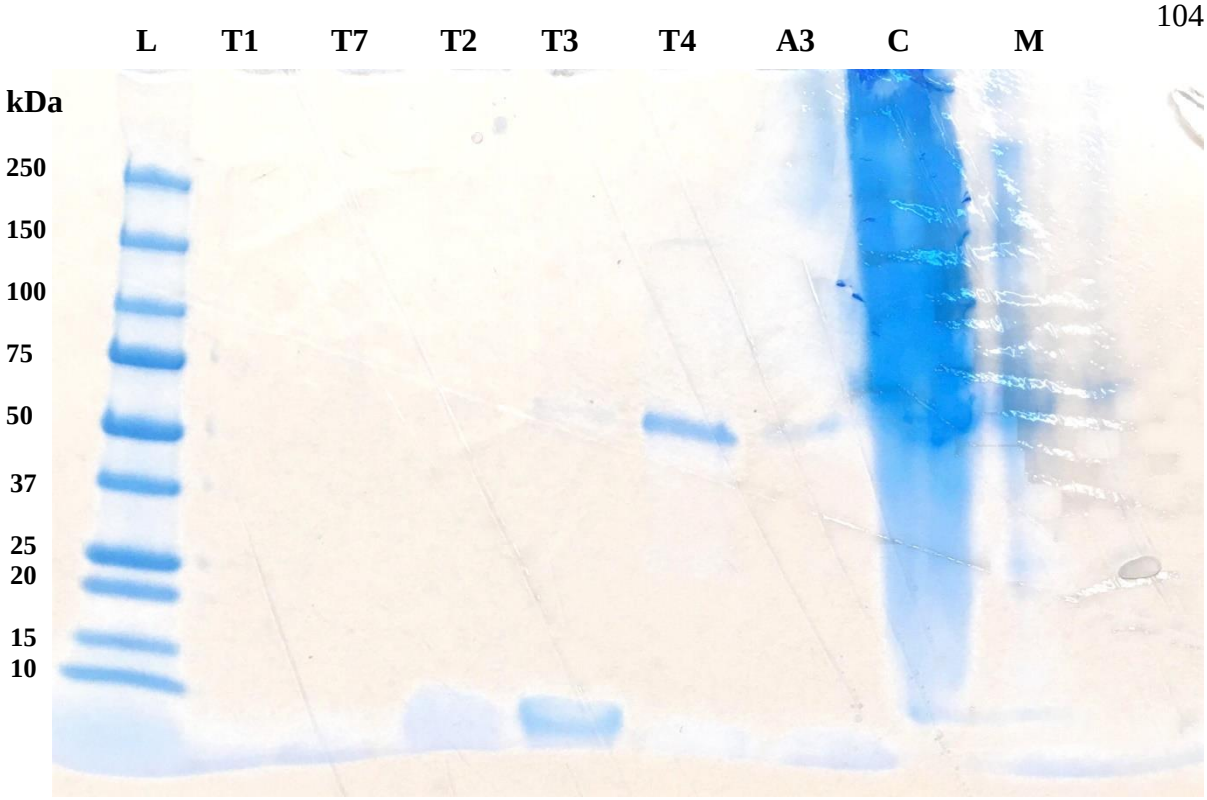

A8. Coomassie Blue staining of SDS-PAGE gel with 10X concentrates of low molecular weight fractions of SDCM, ADCM, M7H9C growth media, and high molecular weight fraction of SDCM. Low molecular weight fractions of SDCM from T1, T2, T3, T4, T7, of ADCM from three-month-old culture, and of M7H9C growth media were lyophilized and resuspended in smaller volume in order to generate 10X concentrates. The samples were loaded on SDS-PAGE gels using Orange G loading dye. The samples were stained with Coomassie Blue stain in order to reveal proteins. **L** – protein standard ladder; **T1, T2, T3, T4, T7** – low molecular weight fractions of SDCM; **A3** - low molecular weight fractions of anaerobically-dormant conditioned media from three-month-old culture; **C** – high molecular weight fraction of SDCM containing molecules above 5kDa in size; **M** - low molecular weight fractions of M7H9C growth medium supplemented with OADC.